FOSSIL IMPRINT • vol. 76 • 2020 • no. 1 • pp. 128–164
(formerly ACTA MUSEI NATIONALIS PRAGAE, Series B – Historia Naturalis)

NATIONAL MUSEUM

CASTOR-LIKE POSTCRANIAL ADAPTATION IN AN UPPERMOST MIOCENE BEAVER FROM THE STANIANTSI BASIN (NW BULGARIA)

THOMAS SEBASTIAN LECHNER[1,2,*], MADELAINE BÖHME[1,2]

[1] Senckenberg Centre for Human Evolution and Paleoenvironment, HEP Tübingen, Terrestrische Paläoklimatologie, Sigwartstraße 10, D-72076 Tübingen, Germany; e-mail: thomas.lechner@senckenberg.de.
[2] Department of Geoscience, University of Tübingen, Sigwartstraße 10, D-72076 Tübingen, Germany; e-mail: m.boehme@ifg.uni-tuebingen.de.
*corresponding author

Lechner, T. S., Böhme, M. (2020): *Castor*-like postcranial adaptation in an uppermost Miocene beaver from the Staniantsi Basin (NW Bulgaria). – Fossil Imprint, 76(1): 128–164, Praha. ISSN 2533-4050 (print), ISSN 2533-4069 (on-line).

Abstract: The Staniantsi-Mazgoš Basin is one of several Neogene intramontane basins in NW Bulgaria. Recent fieldwork in the open pit coal mine yielded material of an exceptional diversity of vertebrates from the uppermost Miocene. In particular, skeletal remains of a large Castorinae are very numerous and well-preserved. Here we perform a comparative morphological description of the postcranium of the Staniantsi-beaver and compare it with the extant *Castor fiber* and closely related fossil taxa, noting an overall high degree of similarity in many cases. Analyses of the functional anatomy confirm similar locomotor adaptations of the large Staniantsi-beaver and the extant *Castor fiber*. It is shown that the hindlimb exhibits typical adaptations for swimming and the forelimb is modified for a primary fossorial movement. Further, the caudal vertebrae indicate a flattened tail. Minor osteological differences can be used in a future clarification of the taxonomic status of this fossil castorine. In conclusion, the large Staniantsi-beaver seems to be equivalent to the extant *Castor fiber* and several fossil castorids in his locomotor adaptations and fits perfectly into the assumed swampy to lacustrine palaeoenvironment of the Staniantsi-Mazgoš Basin. Our results highlight the importance of the postcranium for reconstructing the palaeobiology and elucidating the taxonomy of fossil rodents.

Key words: Staniantsi Basin, Bulgaria, uppermost Miocene, Castoridae, postcranial skeleton, functional morphology

Received: August 4, 2019 | Accepted: July 20, 2020 | Issued: November 9, 2020

Introduction

Although the fossil record of beavers (Castoridae) is extensive, there are many unanswered palaeobiological questions. One of the biggest problems is the insufficient description of the postcranial remains of beavers. So far, taxonomic studies of fossil beavers have relied almost exclusively on the description of cranial material (Korth 2002, Rybczynski 2007). One reason is that many fossil sites do not yield postcranial material and mainly teeth are found. Moreover, the postcranial elements are often not associated with cranio-dental material and thus this material is often neglected. Gerhard Storch has shown that postcranial studies are important for the functional morphology of fossil vertebrates (Schmidt-Kittler and Storch 1985, Habersetzer and Storch 1987, Fejfar and Storch 1994, Storch et al. 1996). Additionally, the postcranium can offer insights into the phylogeny (Felten et al. 1973). Because of the great merit of Gerhard Storch's research to the postcranial skeleton of small mammals, we are pleased to contribute to his memorial volume with a study on the functional morphology of the Staniantsi-beavers.

The taxonomy of Miocene beavers seems to be a "never-ending" problem, which is highlighted by Casanovas-Vilar and Alba (2011). There are very few sites that yield a large enough number of specimens to get at least an idea of the intraspecific variability of fossil beaver populations. Still this variability within one beaver population is unexplored concerning recent beaver populations. To get a clearer view on beaver taxonomy the clarification of this intraspecific variability will be necessary to examine and potentially synonymise confusing fossil taxa.

The site of Staniantsi yields very rich fossil material of beavers, both concerning the quality and quantity of cranial and postcranial skeletal elements. This enables insights into intraspecific variability in a population of beavers from the Miocene. This study is not a taxonomic investigation and it does not aim to describe a new taxon or to revise any other taxa. The objective of this work is to show how postcranial material can provide information on functional morphology and palaeobiology of small mammals. An extensive subsequent publication will concentrate on the

DOI 10.37520/fi.2020.009

cranial remains and combine those with the postcranial morphological results, to achieve a convincing taxonomic conclusion.

Geological setting

The locality of Staniantsi belongs to one of the several small Neogene intramontane basins in Western Bulgaria – the Staniantsi-Mazgoš Basin. The village of Staniantsi is located about 50 km north-northwest of Sofia. The basin measures about 8 km in length and is oriented in a northwest-southeast direction, crossing the Bulgarian-Serbian border (Text-fig. 1).

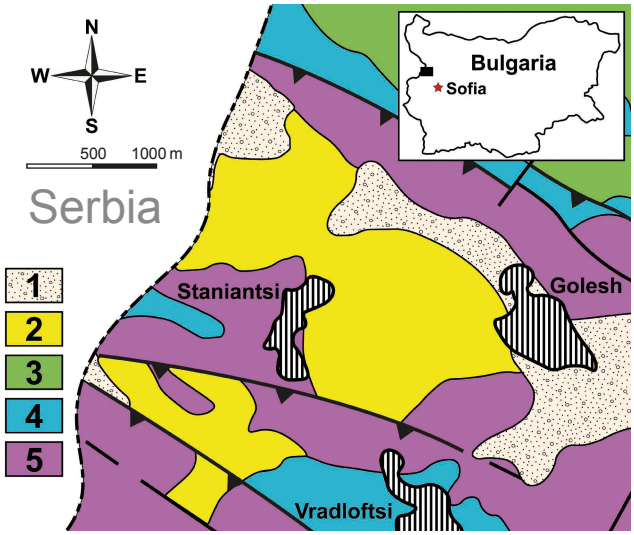

Text-fig. 1. Geological map of the Staniantsi Coal Basin (redrawn from Angelov et al. 1993): 1 – Pleistocene sediments, 2 – Neogen sediments, 3 – Cretaceous sediments, 4 – Jurassic sediments, 5 – Triassic sediments.

The locality is an active brown-coal open-cast mine and exposes a variety of lacustrine to swampy sedimentary facies. Mining activities only take place on Bulgarian territory. Colour-differences in the overview photographs already point to major lithological differences in the sedimentary units (Text-fig. 2).

The basement of the Staniantsi-Mazgoš Basin is built up by Middle Triassic dolomites and Early Jurassic carbonates (Konjarov 1932, Angelov et al. 1993). The Neogene sediments are about 65 m thick comprising lignites, marls as well as blackish to greyish and greenish clays. Three main sedimentary facies can be distinguished (from bottom up): a swamp facies composed of lignites and black clays, followed by lacustrine facies with lacustrine chalk and grey to green marls, superimposed by a terrestrial palaeosol unit with pedogenic carbonates (caliche). All fossil beaver remains come from the swamp facies and the very base of the lacustrine facies.

The stratigraphic age of the section can currently only be determined biochronologically. The fauna contains species typical for both late Miocene and early Pliocene age and may belong to the very late Turolian (uppermost Miocene; see also Utescher et al. 2009, Uhl et al. 2014). The fauna shows a high diversity of vertebrate taxa, containing more than 70 species of all major vertebrate groups (fishes, amphibians, reptiles, birds, mammals) as well as molluscs and botanical components. There is also a diversity in preservation including mostly disarticulated bones as well as rare articulated partial skeletons.

Material and methods

The fossil specimens described herein are housed in the Palaeontological Collection of the University of Tübingen (GPIT). The specimen number is composed of the abbreviation of the collection "GPIT", an acronym for the taxonomic section (e.g., "MA" for Mammalia) and the consecutive number, resulting in a number as GPIT/MA/10660.

Most specimens represent surface findings in the coal pit and the only taphonomical information is usually the stratum they originated from. The abbreviations for the differentiated fossil bearing strata start with 'STA', an acronym for the locality of Staniantsi and are continued by a consecutive number in the order of discovery of that layer. Beavers have been found in STA-2, STA-6 (both swamp unit) and in STA-1 (base of lacustrine unit). All described specimens from Staniantsi are listed in Appendix with their complete supplementary information. Bone preservation is generally very good. Brittle and crumbly bones have been treated with Mowilith (polyvinyl acetate) dissolved in acetone, as a consolidant. Fractures have been stabilised with cyanoacrylate adhesive (super glue) or epoxy resin.

For the comparison of the fossil material of the Staniantsi-beaver two extant skeletons of *Castor fiber* from the Saarland (western Germany) were used. The material is housed in the private collection of the Privates Institut für naturwissenschaftliche Präparation und Forschungssammlung (Nawilab) in Trostberg, Germany. Additionally, a mounted *C. fiber* skeleton of the GPIT was used for comparison.

The anatomical nomenclature primarily follows Schaller (2007), Freye (1954), Landry (1958) and Ginot et al. (2016).

For linear measurements a 150 mm digital calliper with a measurement accuracy of ± 0.03 mm was used. Linear measurements are based on von den Driesch (1976), Elissamburu and Vizcaino (2004), Samuels and Van Valkenburgh (2008). The measurement for calcaneus and astragalus follows Ginot et al. (2016).

The calculation of the intermembral index (IM) and the olecranon length index (OLI) follows Samuels and Van Valkenburgh (2008). The IM indicates the length of the forelimb in relation to the hindlimb. The IM is calculated with the following equation:

$$IM = \frac{\text{Functional length of humerus + Functional lenght of radius}}{\text{Functional length of femur + Functional lenght of tibia}}$$

The OLI indicates the relative mechanical advantage of the muscles used in elbow extension and is calculated with the equation in form of:

$$OLI = \frac{\text{Olecranon process lenght}}{\text{Functional length of the ulna}}$$

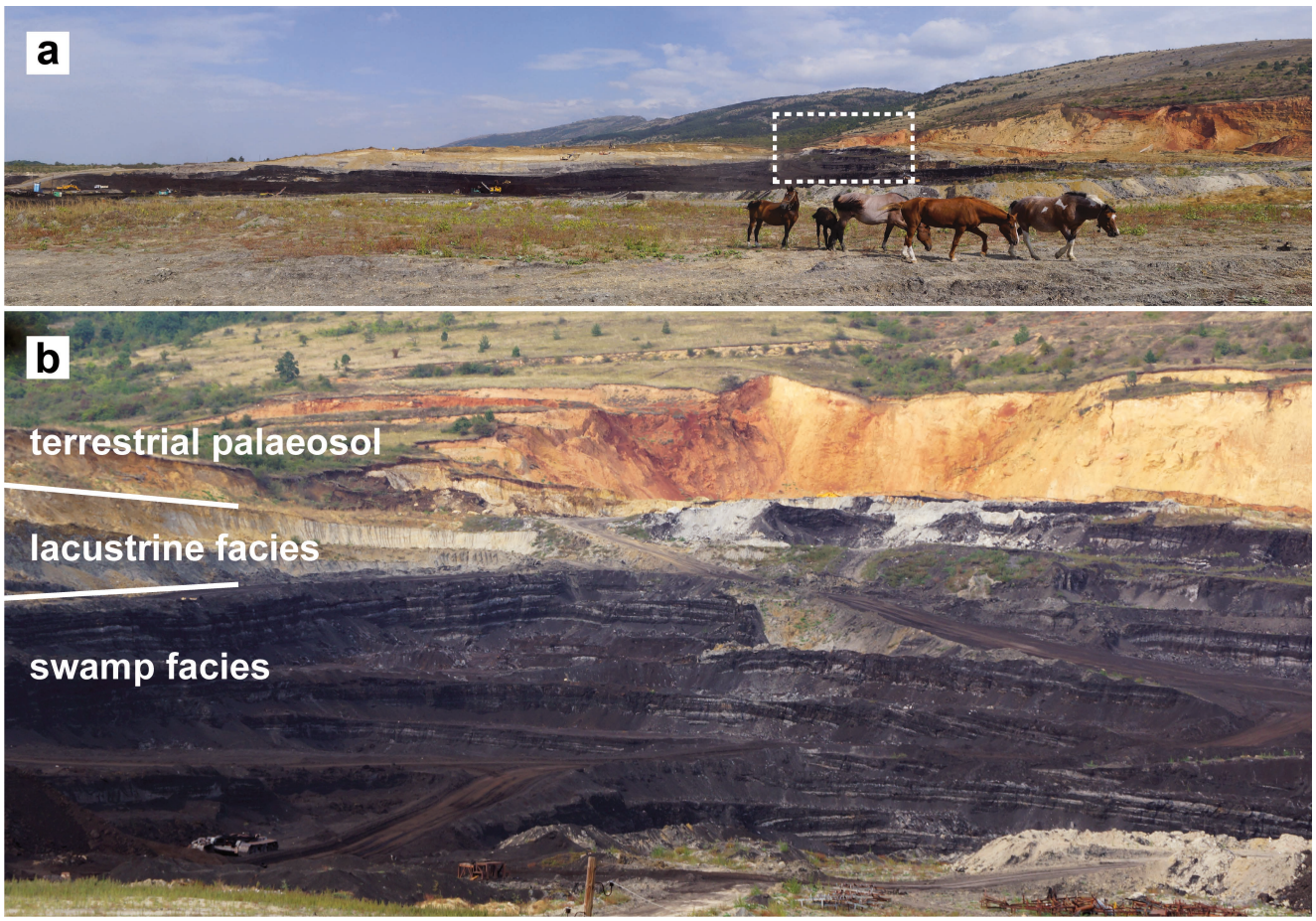

Text-fig. 2. Staniantsi open cast mine seen from south-east (a) and in a more detailed view from the south (b). Most of the studied castorid material originates from the black coal bearing areas (swamp facies).

Furthermore, a calcaneus index (CAI) was calculated. The measurements for this index follow Ginot et al. (2016). The CAI indicates the relative mechanic advantage of the muscles on the Achilles tendon and is calculated with the equation in form of:

$$CAI = \frac{\text{Lenght of the tuber calcanei}}{\text{Length of the calcaneus}}$$

Selection and identification of castorid postcranial bones. Three beaver taxa can be distinguished based on their dental morphology: the minute *Trogontherium* (*Euroxenomys*) *minutum* and the small-sized *Dipoides problematicus*, which both belong to the Castoroidinae and a third, large-sized beaver. The postcranial skeleton of fossil rodents is rarely the main focus of scientific research. Concerning Eurasian fossil beavers, the examination of postcranial material becomes even more difficult. Until now no complete skeleton of a Eurasian Miocene castorine or castoroid has been found. Even from widespread taxa – like *Chalicomys jaegeri* – a complete skull is still lacking (Stefen 2009). Therefore, the question arises, how to distinguish isolated postcranial elements of an animal when the majority of characters are defined in the cranial and only few in the postcranial skeleton. Due to different body sizes of the three taxa, a separation of the postcranial material was possible. One small taxon (approximately the size of a muskrat) most likely represents *Trogontherium* (*Euroxenomys*) *minutum*. A medium sized rodent is the small castorid *Dipoides problematicus*. The large castorid and the porcupine (*Hystrix primigenia*) are representatives for the largest category of rodents in Staniantsi. The large castorid lies in the size range of the extant genus *Castor* (*C. fiber* or *C. canadensis*), whereas the hystricid is slightly smaller in size and can therefore easily be separated. Additionally, the finds of *Hystrix primigenia* are very rare in Staniantsi and limited so far to a single mandible. Robertson and Shadle (1954) provide further information on how to distinguish juvenile castorid bones, with the timing of epiphyseal fusions in bones. The direct comparison with the postcranial material of a recent *C. fiber* leads to a reliable selection of the specimens.

Material

Four anterior caudal vertebrae: GPIT/MA/03822-7 (frag.), GPIT/MA/09409 (frag.), GPIT/MA/09824 (frag.), GPIT/MA/09859-4 lacking left transverse process; medial caudal vertebra: GPIT/MA/09859-3; two posterior caudal vertebrae: GPIT/MA/03851, GPIT/MA/03893 (frag.); five scapulae fragments: left glenoid fossa with coracoid process: GPIT/MA/03819; left glenoid fossa (frag.) with spina scapulae (frag.): GPIT/MA/09858-9; left spina scapulae (frag.): GPIT/MA/09858-15; left glenoid fossa (frag.): GPIT/MA/09855; left glenoid fossa with coracoid process and spina scapulae (frag.) damaged by pyrite decomposition:

GPIT/MA09856; thirteen humeri specimens: right humerus with epiphyses showing an entepicondylar foramen: GPIT/MA/10660; right humerus lacking proximal end and tuberositas deltoidea (frag.): GPIT/MA/09935; left humerus lacking proximal end: GPIT/MA/09931; right humerus diaphysis (frag.) with distal epiphysis: GPIT/MA/09793; right distal humerus (frag.): GPIT/MA/09933; left distal humerus (frag.): GPIT/MA/09941; right distal humerus (frag.) lacking capitulum: GPIT/MA/09858-4; two right humeri diaphysis (frag.) with preserved tuberositas deltoidea: GPIT/MA/09794, GPIT/MA/10668 (frag.); two right humeri diaphyses (frag.): GPIT/MA/03822-1, GPIT/MA/03913; two left humeri diaphyses (frag.): GPIT/MA/09811, GPIT/MA/09823; seven ulnae specimens: left ulna with slightly damaged olecranon, lacking distal epiphysis: GPIT/MA/03758; left proximal ulna (frag.): GPIT/MA/09468; right proximal ulna (frag.) lacking medial olecranon: GPIT/MA/09743; two right proximal ulnae (frag.) with processus anconeus: GPIT/MA/09789, GPIT/MA/03881; left distal ulna (frag.) lacking distal epiphysis (juvenile): GPIT/MA/09968; left ulna diaphysis (frag.) lacking proximal and distal end: GPIT/MA/09964; right radius lacking distal end: GPIT/MA/03822-3; right proximal radius epiphysis: GPIT/MA/09858-3; Manual phalanx distalis of uncertain digit position: GPIT/MA/03841; right innominate bone (frag.) with acetabulum, ilium and pubis, damaged by pyrite decomposition: GPIT/MA/09393; eight femora specimens: right femur lacking epiphysis of trochanter major and medial portion of distal epiphysis: GPIT/MA/09934; three right femora diaphyses (frag.): GPIT/MA/09755, GPIT/MA/09963, GPIT/MA/09858-6; left femur diaphysis (frag.): GPIT/MA/09394; left femur diaphysis, lacking epiphysis (juvenile): GPIT/MA/03882; right epiphysis of a trochanter major: GPIT/MA/10663; left epiphysis of a caput femoris: GPIT/MA/03822-6; seven tibiae specimens: right tibia lacking proximal epiphysis: GPIT/MA/10657; left tibia slightly damaged distally, compressed and damaged proximally: GPIT/MA/09861; right distal tibia (frag.): GPIT/MA/09765; right proximal tibia (small frag.): GPIT/MA/09767; right distal tibia (frag.): GPIT/MA/03822-2; left tibia, heavily fragmented with proximal epiphysis loose (juvenile): GPIT/MA/09858-7; right juvenile diaphysis (frag.): GPIT/MA/09858-8; right distal fibula diaphysis without epiphysis: GPIT/MA/03822-4; left astragalus: GPIT/MA/09796; left astragalus (juvenile): GPIT/MA/09858 1; right astragalus (juvenile): GPIT/MA/09858-2; right astragalus diagenetic compressed (frag.): GPIT/MA/09859; left calcaneus lacking posterior epiphysis: GPIT/MA/10658; right calcaneus (frag.): GPIT/MA/03922; left calcaneus lacking posterior characters (frag.): GPIT/MA/09858-5; tree ossa tarsalia: left os cuboideum: GPIT/MA/09858-10, left os naviculare: GPIT/MA/09858-11, left os cuneiforme III: GPIT/MA/09858-12; five ossa metatarsalia: right os metatarsale V lacking distal epiphysis: GPIT/MA/10659; left proximal os metatarsale IV (frag.): GPIT/MA/09858-13; right proximal os metatarsale IV (frag.): GPIT/MA/09859 5; left proximal os metatarsale III (frag.): GPIT/MA/09858-14; right os metatarsale II lacking distal end (frag.): GPIT/MA/03822-5; two pedal phalanges distales of digit III or IV: GPIT/MA/03889 and GPIT/MA/09951-3.

Comparative description of the postcranial material

In addition to the description of the postcranial material presented here, the fossil site of Staniantsi provides a substantial record of cranial remains. Due to craniodental characters, the Staniantsi-beaver represents a Castorinae Hemprich, 1820 (Rodentia, Castoridae) and is a member of either the genus *Castor* Linnaeus, 1758 or *Chalicomys* Kaup, 1832, which are very complex regarding their taxonomic differentiation. The intention of this paper is not a taxonomic revision but a biomechanical, comparative study of the postcranium of this Castorinae. The measurements taken for several postcranial positions in the Staniantsi-beaver are compared to an extant *C. fiber* in Table 1.

Columna vertebralis

Vertebrae caudalis

Seven vertebrae were identified to belong to the large castorid of Staniantsi (Pl. 1, Figs 2–8). All of these represent caudal vertebrae positions. There are four anterior, one medial and two posterior caudal vertebrae. Most of these specimens pertain to different individuals. The anterior portion of the tail is characterised by prominent transverse processes. These processes cover more than two-thirds of the lateral width of the vertebrae. Unfortunately, nearly all of the large transverse processes are damaged and only the base is preserved. GPIT/MA/09859-4 is the only specimen showing a partly preserved left transverse process (Pl. 1, Fig. 2a–e). Concerning *C. fiber*, the basal characters of the transverse processes are quite similar. Only two vertebrae (GPIT/MA/09859-4 and GPIT/MA/09409) show a preserved neural arch with partial prae- and postzygapophyses (Pl. 1, Figs 2a, b, 5a, d). The very narrow vertebral foramen (spinal canal) in both specimens implies a more caudal position of these vertebrae in the anterior portion of the tail (Pl. 1, Figs 2a, 5a). In contrast to *C. fiber*, in axial view (cranial and caudal) the vertebral bodies of the posterior portion of the tail are not as dorso-ventrally flattened, but are approximately equilateral hexagonal in outline (Pl. 1, Figs 2a, d, 3c, 4b, 5a, b, 6a, b, 7a, b, 8a, b). In the castoroidine *Castoroides ohioensis*, the anterior caudal vertebrae are not flattened dorso-ventrally, while the posterior vertebrae are slightly flattened (Moore 1890). The transverse processes of the posterior vertebrae still occupy half of the width of the vertebrae (Pl. 1, Figs 7d, e, 8d, e). In the anterior portion of the tail, a single process dominates the shape of the transverse processes. The medial and posterior portions of the tail show vertebrae with two transverse processes on each side of the vertebra, comprising one cranially and a smaller one, which is caudally directed. In the larger medial caudal vertebra GPIT/MA/09859-3, these two processes merge into a single, wide cranio-caudally expanded process (Pl. 1, Fig. 4a, c). This character can also be seen in the posterior portion of the tail. In GPIT/MA/03851 this ‘butterfly-shaped’ transverse process is present and the gap between the two initial processes is reduced to a tiny foramen (Pl. 1, Fig. 7d, e). Ventrally, a groove indicates that at least a nerve or a blood vessel passes through this foramen. At the corresponding position in proximal caudal vertebrae with only one large

Table 1. Measurements of the Staniantsi-beaver compared to an extant *Castor fiber* individual from Saarland (Nawilab/1888). Measuring lines follow Samuels and Van Valkenburgh (2008), Moore (1890), Schreuder (1929), Shotwell (1970), von den Driesch (1976) and own (measurements in mm, * approximate values).

Bone type and measurement	Staniantsi-beaver	Staniantsi-beaver	*Castor fiber*
Scapula	**MA/03819**	**MA/09856**	**Nawilab/1888**
Glenoid length	17.7	17.2	19.7
Glenoid width	12.31	11.98	12.5
Humerus	**MA/10660**	**MA/09931**	
Greatest length of humerus	86.5	–	93.3
Midshaft mediolateral diameter of the humerus	11	12	11.1
Length of deltopectoral crest	43	–	47.7
Epicondylar breadth of the distal humerus	36.46	32.9	32.1
Greatest medio-lateral diameter of the epiphysis of the humeral head	22.6	–	25.3
Greatest cranio-caudal diameter of the epiphysis of the humeral head	21.23	–	22.5
Greatest medio-lateral length of the distal joint (trochlea and capitulum)	19.7	19.7	21.5
Greatest cranio-caudal diameter of the distal joint (trochlea and capitulum)	10.4	10.1	10.8
Radius	**MA/03822-3**	–	
Greatest length of the radius	83*	–	97
Greatest length of the radius without distal epiphysis	76	–	89
Greatest medio-lateral diameter of the proximal epiphysis	11.1	–	12.3
Greatest cranio-caudal diameter of the proximal epiphysis	8.1	–	8.2
Ulna	**MA/03758**	**MA/09468**	
length of the ulna	112*	–	129.8
Functional length of the ulna	94*	–	105.5
Functional length of the ulna without distal epiphysis	85	–	95.7
Midshaft mediolateral diameter of the ulna	5.4	–	6.17
Length of the olecranon process of the ulna	20.5	19.5	26.8
Femur	**MA/09934**	**MA/03822-6**	
Greatest length of the femur	122*	–	125
Midshaft anteroposterior diameter of the femur	12.5	–	12.5
Height of the greater trochanter of the femur	16*	–	18
Epicondylar breadth of the distal femur	40.5*	–	42.2
Diameter of femoral head	15.2	16.5	17.7
Tibia	**MA/10657**	**MA/09765**	
Greatest length of the tibia	147*	–	145.3
Greatest length of the tibia without proximal epiphysis	142.5	–	138
Midshaft mediolateral diameter of the tibia	12.5	12.5	12.38
Length of tibial tuberosity	85*	–	85
Length of tibial tuberosity without proximal epiphysis	73	–	71.5
Greatest medio-lateral diameter of distal epiphysis	19.8	22.7	21.8
Greatest cranio-caudal diameter of distal epiphysis	19.5	22.1	17.5
Astragalus	**MA/09796**	**MA/09858-1/2**	
Astragalus total width (medio-lateral)	23.7	20.9	22.5
Astragalus total length (proximo-distal)	25.6	23.6	23.8
Astragalus body width (medio-lateral)	23.5	20.2	22.4
Lateral trochlea length (proximo-distal)	17.8	15.2	13.9
Astragalus total hight (dorso-plantar)	15.4	12.7	14.1
Astragalus head hight (dorso-plantar)	8.5	6.6	8.8
Astragalus head width (medio-lateral)	13.6	11.6	13.1
Calcaneus	**MA/10658**	–	
Calcaneus posterior length (length of tuber calcanei)	22.3	–	30.7
Calcaneus total length	48.2	–	56
Calcaneus total width	29.1	–	25.5
Tuber calcanei hight (dorso-plantar)	12.4	–	11.9
Maximum height (dorso-plantar)	18.2	–	16.5
Phalanx	**MA/03889**	–	
Greatest length of terminal pedal phalanx of digit III or IV	17.3	–	18.9
INDEX Calculations	**Staniantsi-b.**	–	***Castor fiber***
CAI (Calcaneus index) of GPIT/MA/10658	0.46	–	0.55
IM (Intermembral index) of combined individuals	0.63	–	0.7
OLI (Olecranon length index) of combined individuals	0.22	–	0.25

transverse process a sulcus is visible. The groove passes ventrally around the caudal margin of the transverse process and continues at the dorsal surface until it proceeds through a lateral foramen, penetrating the neural arch. Even in the smallest vertebra (GPIT/MA/03893) this foramen is present, but due to the poor state of preservation it is not completely preserved (Pl. 1, Fig. 8c–e).

Forelimb

Scapula

Five specimens represent scapulae (Pl. 2, Figs 3, 4). In four of them only the proximal part is preserved. On some specimens, further features are observable, but all of them are poorly preserved. One specimen represents a fragment of the scapular spine.

For a better understanding of the description of the scapula, the anatomical terms used are indicated in Text-fig. 3.

In proximal view, the glenoid cavity (cavitas glenoidales) is cranio-caudally concave and the outline is horizontally pear-shaped with the narrow end pointing cranially. In the castoroidine *Trogontherium cuvieri* the glenoid cavity is of equal length to that of the castorines *C. fiber* and the Staniantsi-beaver but broader (Schreuder 1929: pl. X, figs 13c, 15b). This means, that in the castorines, the humeral head is broader than the glenoid cavity of the scapula (Schreuder 1929). Ratio specifications for the glenoid, given by Schreuder (1929), are 11:7 for *C. fiber*, which is the same in the extant *C. fiber* (Nawilab/1888) specimen, and 11:8 for the castoroidine *Trogontherium cuvieri*. Moore (1890) reports a ratio of 11:7 for *Castoroides ohioensis* which perfectly matches the ratio of the other castorines. In the fossil Staniantsi-beaver the ratio is 11:7.6 (GPIT/MA/3819: 17.7 mm : 12.3 mm; GPIT/MA/9856: 17.2 mm : 12 mm), which lies in-between those values. The posterior portion of the glenoid cavity is nearly circular, whereas the cranial margin is very elongated and bent in cranio-distal direction, forming a distinct coracoid process (processus coracoideus). On the lateral margin of the coracoid process, the supraglenoid tuber is represented by a shallow elevation. The coracoid process is very similar to that of *C. fiber* but in the latter, the process terminates more sharply and blade-like and is elongated medially. As described by Schreuder (1929): "in the castoroidine *Trogontherium cuvieri* the coracoid process […] is shorter, broader and less curved". The neck of the scapula has half of the width of the distal glenoid. The cranial margin of the neck merges with the distal surface of the coracoid process, the caudal margin runs parallel and has a tuberous surface structure. The lateral neck, joins with the edge of the scapular spine (spina scapulae) and raises in a circular path. Compared to *Castor*, this character indicates a very dominant and extended acromion of the scapular spine.

Humerus

Thirteen humeri are present (Pl. 3, Figs 1–3, Pl. 4, Figs 1, 2). Only one specimen is preserved entirely. A second humerus is proximally fractured in half without any clear fit. Two more humeri were found without the proximal joint but show a well-preserved distal epiphysis that is seamlessly fused with the diaphysis. Furthermore, there are three distal ends whereas one has a well-preserved trochlea and capitulum and the others represent only joint fragments. Subsequently there are six diaphysis-fragments without any articular surfaces. Most of the anatomical terms used in the description are indicated in Text-fig. 4.

The caput humeri (humeral head) is slightly angled caudally, but to a lesser extent than in *C. fiber*. The caput humeri of the Staniantsi-beaver and *C. fiber* are approximately

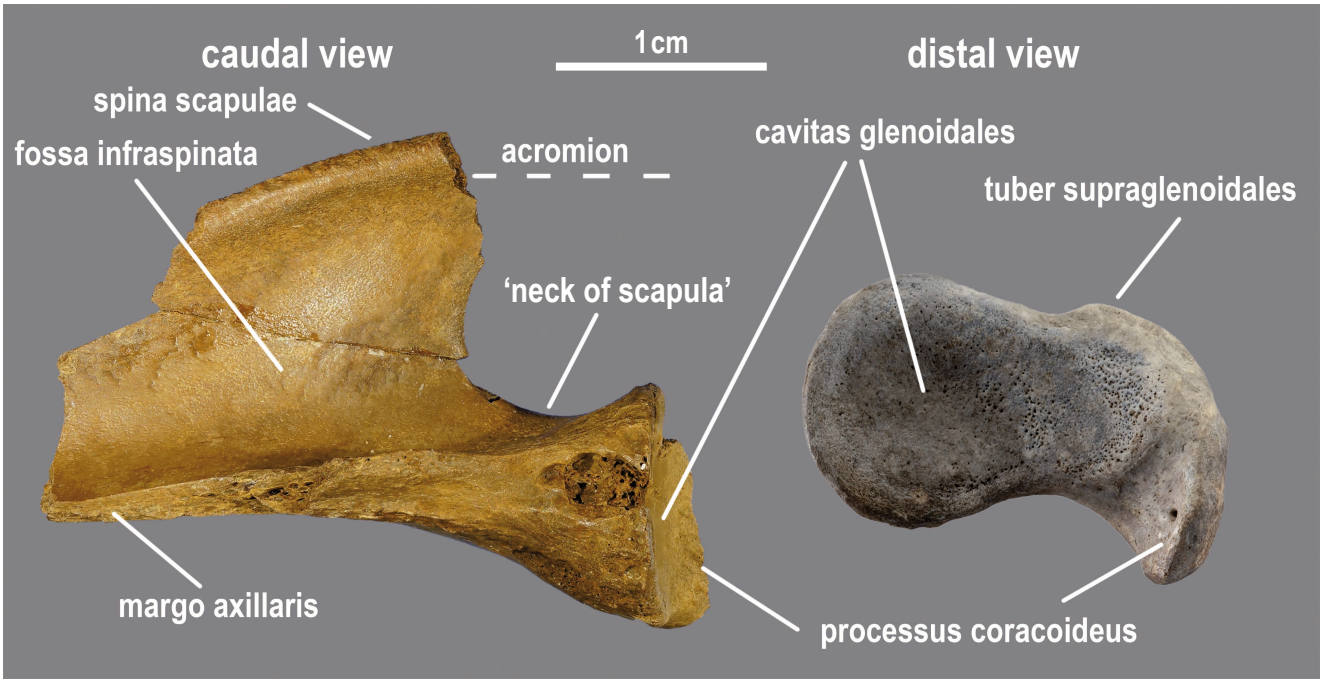

Text-fig. 3. Right scapula of the large Staniantsi-beaver in caudo-lateral and distal view with markings of the anatomical terms used for the description of the scapula. Left figure: caudal view of GPIT/MA/09858-9. Right figure: mirrored distal view of GPIT/MA/03819.

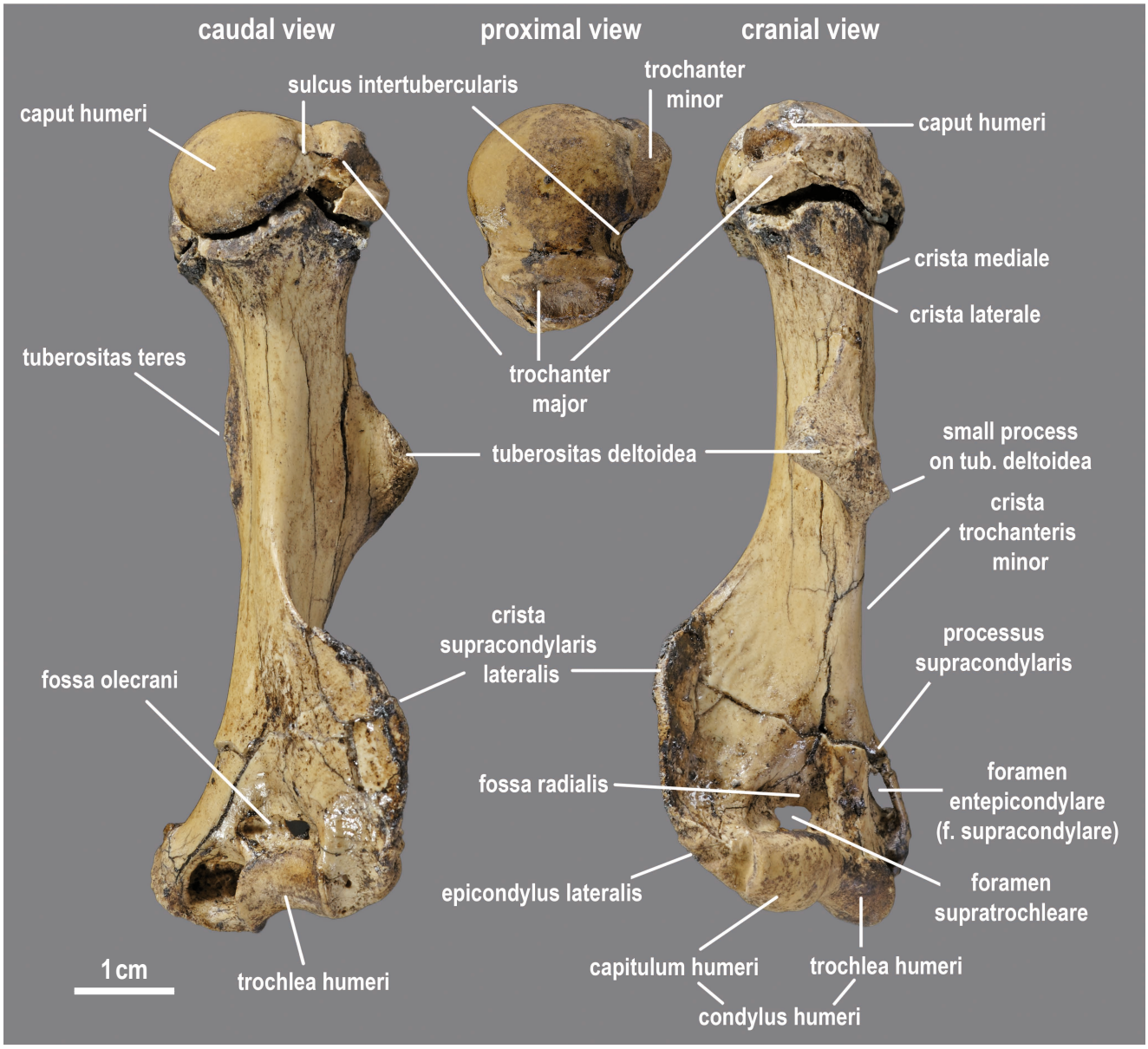

Text-fig. 4. Right humerus of the large Staniantsi-beaver (GPIT/MA/10660) in caudal, cranio-lateral and proximal view with markings of the anatomical terms used for the description of the humerus.

equal in cranio-caudal length and medio-lateral width. In the castoroidines e.g., *Trogontherium cuvieri* the humeral head is longer (cranio-caudal) than wide (Schreuder 1929). The trochanter major (greater trochanter) and the caput humeri are of equal height, unlike *C. fiber*, where the greater trochanter is higher and separated from the humeral head by a sulcus (groove). Furthermore, the trochanter major is extending more cranially than *C. fiber*, but overall, it is cranio-laterally oriented. The trochanter minor (lesser trochanter) is lower than the caput humeri, as in *C. fiber* and transitions into the head without any well-marked groove. In contrast, castoroidine beavers show a well-marked sulcus that separates the trochanter minor from the caput humeri e.g., *Procastoroides* (Shotwell 1970), *Castoroides* (Moore 1890) and *Trogontherium cuvieri* (Schreuder 1929).

The proximal portion of the diaphysis of the Staniantsi-beaver is nearly as long (antero-posteriorly) as wide (medio-laterally). Whereas, in *C. fiber* the width (medio-laterally) is almost twice as great as the length (antero-posteriorly). Thus, the cross section forms an acute-angled triangle with a medially pointing tip in *C. fiber*. In the Staniantsi-beaver this triangle is almost equilateral. In the castoroidines *Castoroides*, *Trogontherium cuvieri* and *Procastoroides*, the proximal portion of the humerus diaphysis is wider than long, as in the case of *C. fiber* (see Moore 1890, Schreuder 1929, Shotwell 1970). The medial and lateral cristae fuse to form the triangular tuberositas deltoidea (deltoid tuberosity) halfway to the distal end of the humerus. This tuberosity starts pointing laterally and as it extends flips slightly over pointing latero-caudally, forming a groove. This deltoid tuberosity is typical for both Castorinae and Castoroidinae (Schreuder 1928b, Shotwell 1970). The shape of the crista lateralis at the proximal deltoid tuberosity is varying from convex to concave in different specimens (convex: GPIT/MA/9931, see Pl. 3, Fig. 1a, e; straight: GPIT/MA/09794; concave: GPIT/MA/10660, see Pl. 4, Fig. 1c, d). Additionally, a very small process starts in the distal half of the deltoid tuberosity pointing cranio-medially.

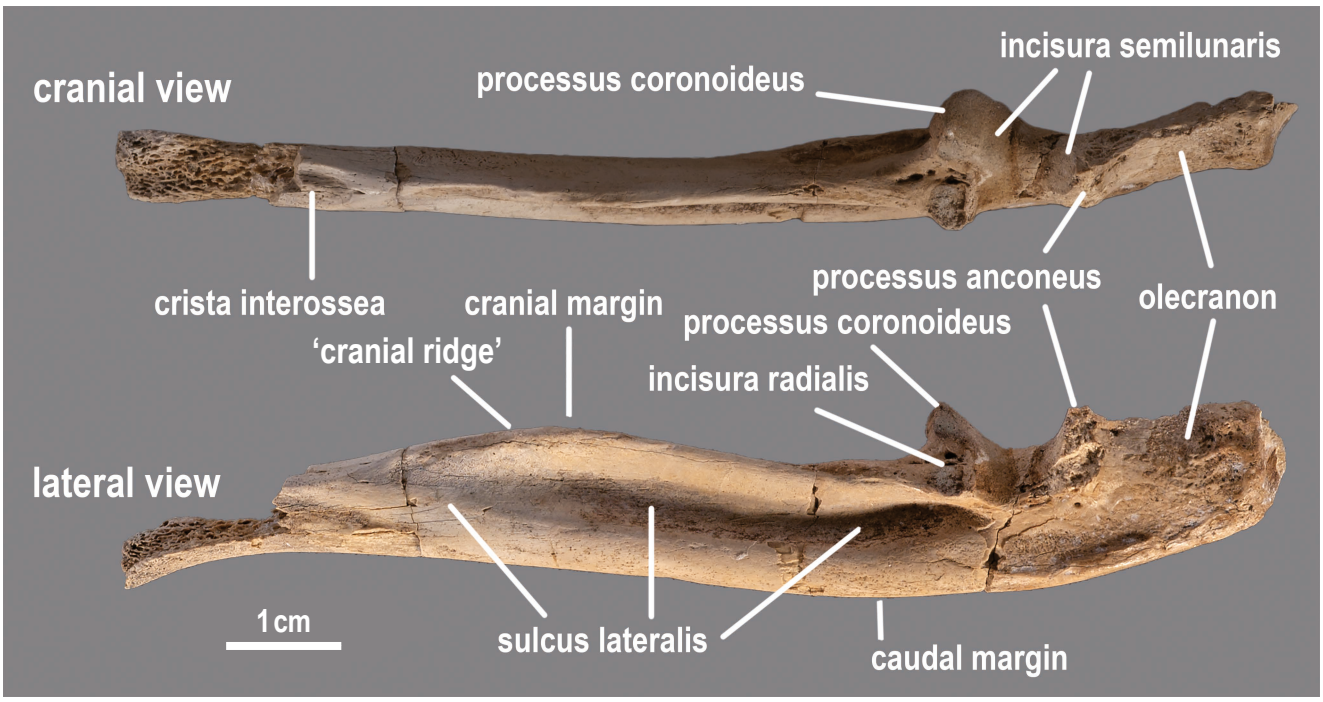

Text-fig. 5. Left ulna of the large Staniantsi-beaver (GPIT/MA/03758) in cranial and lateral view with markings of the anatomical terms used for the description of the ulna.

In the available *C. fiber* material this tiny process is barely perceptible, but present. Directly below the deltoid tuberosity the cross section of the shaft forms an equilateral triangle just like in *C. fiber*. The crista supracondylaris lateralis (supracondylar ridge) starts in the middle of the diaphysis of the humerus, approximately at the height of the distal deltoid tuberosity, and extends laterally to the epicondylus lateralis, taking a convex shape. The proximal orientation varies from a caudal, with a long helical pathway, (GPIT/MA/09931) to a nearly lateral direction (GPIT/MA/10660) leading to a very flat distal humerus. *Castor fiber* follows this second description with a cranio-caudally flattened distal humerus and the crista supracondylaris lateralis reaches a maximum lateral extension at the level of the fossa radialis. In the Staniantsi-specimens the maximum extent of this crista is already reached halfway between the tuberositas deltoidea and the end of the condylus humeri. In castoroidines this peak of lateral extension is placed within the distal one-third of the crista supracondylaris (see Moore 1890, Schreuder 1929, Shotwell 1970). Furthermore, this crista is protruding more laterally in the Staniantsi-specimens than it does in the case of *C. fiber*. If one puts a line from the lateral end of the trochanter major to the lateral edge of the trochlea humeri in *C. fiber* the crista supracondylaris lateralis is only just overtopping this line whereas it is protruding more than five millimetres in the fossil specimens from Staniantsi. The fused lateral/medial crista extends distally from the tuberositas deltoidea in a straight torus to the trochlea humeri. Due to the width of this torus (reaches width of the trochlea humeri) there is no real fossa coronoidea, but a very tiny and flat cavity without conjunction to the fossa radialis. The fossa radialis is present in a way that is comparable in depth and lateral expansion to the *C. fiber* material. Whereas, *C. fiber* shows a very distinctive fossa coronoidea in fusion with the fossa radialis. Starting at the trochanter minor (proximal portion of the humerus), as in *C. fiber*, the crista trochanteris minor is protruding distally, but not nearly as distinctive. In the fossil specimens this crista is more similar to a torus than to a thin and off-standing crista as it is in *C. fiber*. In either case at the level of the tuberositas deltoidea there is a tuberositas teres (teres tuberosity) that is smaller in the specimens of Staniantsi. In both, the tuberositas is pointing to medio-caudal and sometimes flipping caudally. The epicondylus at the medial humerus (medial epicondyle) is also very distinctive and ends in a small spur (processus supracondylaris) pointing proximally. Although this spur in *C. fiber* is more distinctive, there is one fossil specimen (GPIT/MA/10660) showing a protruding bony conjunction to the humeral diaphysis, building a foramen entepicondylare (see Pl. 4, Fig. 1a–c and Text-fig. 4). Of all the humeral specimens this is the only one showing such a highly developed foramen. The occurrence of an entepicondylar foramen seems to be constant in the castoroidine *Trogontherium cuvieri* (Schreuder 1929), while lacking in *Procastoroides* (Moore 1890). It occurs irregularely in castorines as *Steneofiber viciacensis* (Filhol 1879, Schreuder 1928b) and is known from *Steneofiber depereti* (see Gervais 1869) and *Palaeocastor* (see Schreuder 1929). The distal condylus humeri articulates with the radius and ulna in a well-developed hinge-joint. The morphology of this joint is similar to that of *C. fiber* and includes a helical torsion. The fossa olecrani at the distal caudal humerus is distinct and equivalent in latero-medial breadth to *C. fiber*. In two specimens it is penetrated and forms a foramen supratrochleare (GPIT/MA/10660 and GPIT/MA/09933). On the caudal portion of the humerus, medial to the trochlea humeri, there is a deep fossa undermining a huge part of the medial epicondylus from the caudal, distal humerus. In a medial view, it is visible that in *C. fiber* the humerus is angled caudally from the middle of the shaft towards the

proximal epiphysis. This feature is absent or only very slightly observable in the specimens from Staniantsi. In *C. fiber* this angle, which is not well quantifiable due to the cristae and tuberosities, ranges approximately from 20° to 30°.

Ulna

Seven specimens represent ulnae (Pl. 5, Figs 1–4). One nearly complete ulna is just lacking the distal end. Four specimens represent proximal portions. In all of these the olecranon process is marginally damaged. Furthermore, two pieces represent diaphysis fragments with neither epiphyses nor joints. Most of the anatomical terms, used in the description are illustrated in Text-fig. 5.

The ulna of the Staniantsi-beaver has many similarities with *C. fiber*. In the Staniantsi-beaver the olecranon is about one-fifth (0.2) of the functional length of the ulna (olecranal index, OLI). The extant *C. fiber* (Nawilab/1888) reaches values of 0.2–0.25. Different OLI data for fossil beavers are provided by Samuels and Van Valkenburgh (2008). Most of those fossil taxa match the values of the Staniantsi-beaver and the extant *Castor*: *Castoroides ohioensis* (0.22), *Castor californicus* (0.25), *Dipoides stirtoni* (0.25) and *Procastoroides idahoensis* (0.25). Only *Palaeocastor nebrascensis* (0.30) and *P. fossor* (0.31) show slightly higher ratios what stands for an elongated olecranal process compared to the ulna length. Due to the helical rotation of the humeral joint and similar to extant beavers the proximal ulnar joint is asymmetrical in shape. For this purpose, the coronoid process is shifted medially, whereby the incisura radialis occupies the cranio-lateral position in the joint area. The incisura semilunaris covers all of the internal processus anconeus and most of the processus coronoideus. Another trait shared with *C. fiber* is the incisura semilunaris that covers, in addition to the medial processus coronoideus, the lateral part proximally to the incisura radialis. In the castoroidine *Trogontherium cuvieri*, the incisura semilunaris does not cover this portion proximally to the incisura radialis and the articulation with the humerus lies on the small medial wing of the coronoid process (Schreuder 1929). Followingly, the anterior distal joint of the humerus is wider in *Trogontherium* than in *Castor* and the Staniantsi-beaver. Moreover, the anterior trochlea of the humerus is smaller in those castorines than in the castoroidine *Trogontherium*. In *C. fiber* there is a deep groove on the proximal medial surface of the olecranon. The two available Staniantsi-specimens representing this portion show in one case a very shallow and in the other a slightly deeper groove in this position. Subsequently, the olecranon is very narrow in latero-medial direction in contrast to *C. fiber*. In lateral view, the ulna of the Staniantsi-beaver is sigmoid-shaped, with the olecranon pointing cranially and the distal portion pointing caudally. In respect to this, the distal ulna of *C. fiber* is nearly straight and in contrast to the Staniantsi-beaver, the proximal ulna is pointing caudally. In cranial view, the ulna is shaped like a flat arc in medial direction. The lateral ulna is dominated by a strongly marked, longitudinal fossa (sulcus), starting slightly proximal to the incisura radialis and protruding in a straight line parallel to the caudal ridge of the ulna. This is typical for many castorines and castoroidines (Moore 1890, Schreuder 1929). In contrast to *C. fiber* where the sulcus lateralis and the cranial ridge is parallel and straight, the only Staniantsi-specimen showing this area (GPIT/MA/03758) exhibits a convex outline of the cranial ridge with a maximum extension at about the middle of the shaft of the ulna (see Pl. 5, Fig. 1a, c, Text-fig. 5). With regard to the cranial ridge, the castoroidine *Trogontherium cuvieri* follows the traits of *C. fiber* (see Schreuder 1929: pl. XI). In the distal third of the ulna of the Staniantsi-specimen, the sulcus lateralis flattens and merges into a crista interossea. This crista is a contact area to the distal radius. Unfortunately, so far there is no undamaged distal ulna from Staniantsi whereby a further description of the distal joint could be provided.

Radius

The morphology of the radius (Pl. 2, Figs 1, 2) differs in some points to the radius of the extant *C. fiber*. The radius is distinctly convexly curved lengthwise with the proximal and distal end pointing caudally. In *C. fiber*, the shaft is almost straight. This cranially convex radial diaphysis is the counterpart of the convex shape of the cranial ridge of the ulna. The castoroidine beavers *Castoroides* and *Trogontherium* have a slightly curved radius similar to that of *C. fiber* (Moore 1890, Schreuder 1929). In GPIT/MA/03822-3 the proximal epiphysis is already sutureless fused with the diaphysis (Pl. 2, Fig. 1a–d), whereas the distal epiphysis is still unfused. This is clearly recognizable by the tuberous margin of the distal diaphysis. Unfortunately, most of the distal end is damaged. The order of suture fusion is similar to that of the other castorids (Filhol 1879, Schreuder 1929, own observation) and the castoroidine *Trogontherium* (Schreuder 1929). On the caudal side of the proximal epiphysis, the radius joins the ulna with a small, slightly convex facet. Due to the almost straight surface this joint scarcely allows smooth rotary motions. The lateral margin of the radial epiphysis is perpendicular to this base line. In *C. fiber* the outline of the proximal epiphysis of the radius is almost elliptical. Additionally, the castoroidine *Trogontherium* shows no right angle (Schreuder 1929). The connection between these medial and cranial corner-points forms a consistent, cranio-medially convex arc. The latero-medial width of the proximal epiphysis is wider than the cranio-caudal length as in other castorines and castoroidines (Schreuder 1929). The proximal radius is flattened in aspect of the caudal (ulnar-directed) surface. Approximately starting after the proximal third the diaphysis is twisted counter-clockwise until a distal angle of about 45° is reached. The diameter of the distal radius significantly increases until the distal termination is reached. Contrary to the ulna, the radius is distally larger than proximal.

Manus

The only found specimen that can be located in the manus is a phalanx distalis of uncertain digit position (Pl. 12, Fig. 4a–e).

Due to the lack of any physical information for other bones of the hand even the assignment of the phalanx remains uncertain. The available distal phalanx is very narrow in latero-medial extension. Nevertheless, the phalanx is longitudinally extended, dorsal strongly convex and

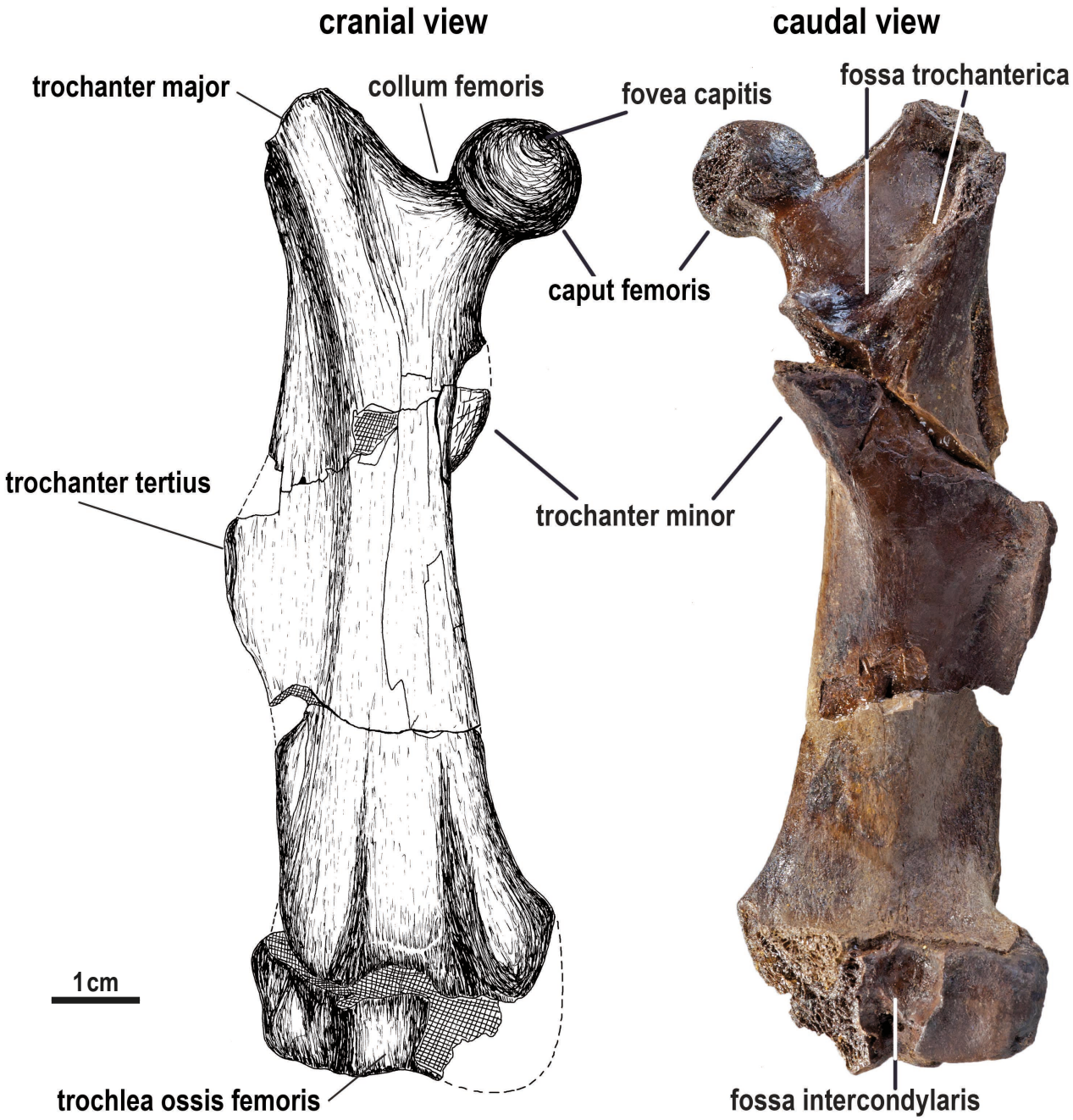

Text-fig. 6. Right femur of the large Staniantsi-beaver (GPIT/MA/09934) in cranial and caudal view with the illustration of the anatomical terms used for the description of the femur. Drawing: T. Lechner.

plantar flattened. The diameter in dorso-palmar direction is nearly as large as the latero-medial one. In the extant *Castor* the distal phalanges of the manus are smaller and slenderer than the pedal ones. This leads to the conclusion that the specimen belongs to the manus and not to the pes.

Hindlimb

Innominate

One right innominate bone fragment consisting of a partly preserved acetabulum, parts of the ilium and pubis represents the only pelvis fragment (Pl. 6, Fig. 1a–c). Due to pyrite decomposition the specimen is difficult to study.

Morphologically, the preserved innominate fragment is quite similar to the extant *Castor* material. In cross section, the ilium is triangular in shape. At a distance of 35 mm from the acetabulum as compared by Schreuder (1929), the cross section is quite similar to that of *C. fiber*. It seems to be typically in this section for the castorines to have a triangular section wider (medio-lateral) than high (dorso-ventral). This relation is reversed in the castoroidine *Trogontherium cuvieri* (Schreuder 1929: fig. 7). The medial surface of the ilium is covered by the articulatory surface (facies auricularis) to the sacrum (articulatio sacroiliaca). The dorsal margin of the ilium is anteriorly very rounded and smooth at the acetabulum. At the caudal border of the auricular surface the beginning of a sharp dorsally pointing crest is initiated. This crest parallels the sacroiliacal articulation in cranial direction. The lateral pars iliaca is divided into a dorsal and a ventral surface. A crest (margo lateralis) centred on the

lateral side of the ilium originates at the cranial margin of the acetabulum and runs cranially. In the extant *Castor* this crest runs until the edge of the ilium (linea iliaca), but due to breakage this cannot be compared to the Staniantsi-beaver and this course cannot be proofed yet. Unfortunately, the caudal innominate is also lost due to breakage. Nevertheless, the preserved part of the acetabulum is very deep and nearly hemispherical, as it is typical for other castoroidines and castorines (Moore 1890, Schreuder 1929). Furthermore, the acetabular notch (incisura acetabuli) is oriented caudo-ventrally and opens the lunate surface. Only a part of the ischium and pubis is involved in this notch. Ventral to the acetabulum is the ventrally-oriented iliopubic eminence (eminentia iliopubica) as a result of the merging caudal ilium and the distal pubis.

Femur

Eight femora specimens are available (Pl. 6, Fig. 2, Pl. 7, Figs 1–4). There is one well-preserved femur of a large adult individual (GPIT/MA/09934), that is used for the primary description. Three large diaphyses probably also represent adult animals. Additionally, there is one large seceded epiphysis of a greater trochanter and one epiphysis of a femoral head. Two diaphyses, one of an intermediate size and one of a very small size seem to represent juvenile or subadult individuals. Most of the anatomical terms, used in the description are illustrated in Text-fig. 6.

The femur is very flattened cranio-caudally and shows sharp crests and processes. The main shaft is medio-laterally extended. The cortical bone of the shaft is very robust (observable in the cross section of damaged specimens). The caput femoris is clearly separated from the shaft. The neck (collum femoris) is flattened cranio-caudally. The fovea capitis, the attachment point of the ligamentum teres, is clearly visible. The caput femoris is pointing cranio-medially. The proximal margin of the femur is characterised by a latero-distally oriented ridge, building a small portion of the femoral neck, before it expands back in latero-proximal orientation forming the trochanter major (greater trochanter), forming a hockey-stick-shaped or V-shaped incision, viewed cranially. In *C. fiber*, the incision between the greater trochanter and the femoral head is hollowed out widely, forming a U-shape. In this respect, the femur of the fossil castoroidines *Trogontherium cuvieri* and *Castoroides ohioensis* show a smooth and deep U-Shape (Moore 1890, Schreuder 1929, Mol and de Vos 1995). In the castoroidine *Procastoroides* the incision is shallow U-shaped (Shotwell 1970). *Steneofiber depereti* and *S. viciacensis* reach an intermediate state, being most comparable to the Staniantsi-specimens (Schreuder 1928b). The proximal femur is dominated by the trochanter major, which protrudes further in proximo-lateral direction and overtops the femoral head. Ventral to the neck a depression (fossa trochanterica) appears reaching the deepest carved point on the ventral centre of the trochanter major. Here the extension is limited by a ridge starting at the proximo-lateral trochanter major proceeding in an arch-shape to the disto-medial end. At this position the proximal margin of the trochanter minor (lesser trochanter) is located. The trochanter minor points slightly ventrally, but maintains a primarily medial tendency. The caudal trochanter minor is clearly structured with small pits. In the extant *Castor* at the trochanter major two lateral edges start protruding distally. By contrast, with the Staniantsi-beaver one of these ridges is shifted to the cranial aspect of the femur and forms a bulge rather than an edge. This bulge seamlessly blends into the central, cranial shaft. In *C. fiber* the second edge is located at the very caudal margin of the lateral aspect. In contrast to the Staniantsi-specimens, which show in lateral view, an edge that is almost shifted to a centred position. A ridge extends from the distal margin of the trochanter major, the lateral-most expansion is reached halfway along the shaft, forming the trochanter tertius (third trochanter). Proximal to the third trochanter the ridge declines until the distal end of the femur. The trochanter tertius and a large part of the edge are bending caudally building a longitudinal overhang. The lateral portion of the diaphysis is caudally concave to sigmoidal impressed and not planar to convex, as it is in *Castor*. Above all, this difference is based on the lateral ridge and the trochanter tertius of the femur, that is forming an overhang in caudal direction. The cranial shaft, neglecting the lateral and medial trochanters and crests, is more or less drop-shaped in cross section. In *C. fiber* the trochanter tertius is very pronounced and characterised by a proximo-distally restricted extent. The trochanter tertius is positioned more distally to the lesser trochanter in the Staniantsi-beaver and the other Castorinae (*Castor*, *Chalicomys*, *Steneofiber*) (Filhol 1879, Schreuder 1928b, Stefen 1997, Daxner-Höck 2004, Casanovas-Vilar et al. 2010). In the Castoroidinae beavers (*Dipoides*, *Procastoroides*, *Castoroides*, *Trogontherium*) the trochanter tertius is directly situated opposite to the lesser trochanter (Moore 1890, Schreuder 1928a, b, 1929, Schotwell 1970). The tree trochanters (major, minor and tertius) form a right-angled-triangle where the hypotenuse touches the two lateral trochanters (t. major and t. tertius). In *Castor* the medial margin of the distal femur is dominated by a medial edge that starts at the trochanter and proceeds until the distal end of the femur. The Staniantsi-specimens show something different. Although the trochanter minor significantly overtops the medial margin, the distal running edge vanishes very early, approximately at the height of the maximum extension of the trochanter tertius. Instead of this edge, the medial distal margin of the shaft is rounded and smooth. The lateral femur is restricted by the edge building up the trochanter tertius. This leads to a drop-shaped cross-section of the distal diaphysis. The distal epiphysis of the femur and the articulation facets are very similar to the extant beaver. GPIT/MA/09934 is the only femur with a partly preserved distal epiphysis (Pl. 6, Fig. 2a–f and Text-fig. 6). Unfortunately, only the lateral portion of the epiphysis is preserved and can be described. The rest of the epiphysis is lost due to breakage. The distal portion of the femur is laterally widened. On the cranial surface of the distal epiphysis the trochlea ossis femoris (patellar groove), the articulation facet for the patella is located. This facet is cranio-distally lifted and is slightly pointing laterally. Caudally, the fossa intercondylaris, in the line of the patella articulation, divides the lateral and medial condyles from each other. The lateral condyle forms a saddle-joint and is slightly tilted medially. Furthermore, the saddle-shaped facet does not reach a rectangular orientation to the distal

shaft and extends between a caudo-proximal and caudo-distal direction. In the juvenile specimens nearly all the described features are already observable in an at least moderate expression. The smallest femur GPIT/MA/03882, shows a very good preservation with all epiphyses in an unfused stage (Pl. 7, Fig. 4a, b). The parting lines of the epiphyses are all present and nearly undamaged, but the epiphyses are lost. It is noted that in the largest, most probably adult femur specimen (GPIT/MA/09934), the epiphysis of the trochanter major as well as the distal epiphysis remain still unfused to the shaft bone and show a suture-line. While, the epiphysis of the femoral head is seamlessly fused to the diaphysis.

Tibia

There are seven specimens representing tibiae (Pl. 8, Figs 1–4, Pl. 9, Fig. 1). The main description follows the best-preserved tibia that lacks only the proximal epiphysis (GPIT/MA/10657). Furthermore, there are three fragments representing at least the distal tibia. On some of them also a greater portion of the diaphysis is observable. There is one fragment of a proximal epiphysis. Finally, there are two very heavily fragmented tibiae representing a juvenile beaver (none of the epiphyses is seamlessly fused to the shaft). The distal epiphysis of most of the tibia-specimens are seamlessly grown together with the diaphysis, corresponding to subadult or adult individuals (Freye 1954). Nevertheless, no proximal epiphysis is ancylosed. Schreuder (1929) already mentioned "this epiphysis appears to ancylose very late with the shaft" in the Castoroidinae *Trogontherium cuvieri*. The bones of the juvenile individual-complex have still unfused epiphyses (GPIT/MA/09858-7 and GPIT/MA/09858-8). Most of the anatomical terms, used in the description are illustrated in Text-fig. 7.

In lateral view, the tibia is sigmoidal in shape. The proximal portion of the tibia is tilted caudally. Two facets for articulation, the medial and lateral condyles compose the proximal epiphysis. As in the extant beaver, the medial condyle is concave in shape and the proximal condyle is convex in cranio-caudal direction. The proximal diaphysis of the tibia is dominated by three crests (crista medialis, c. interossea and c. tibiae) giving it a T-shaped cross section. In *C. fiber* and the Staniantsi-beaver the crests are approximately of equal dominance. In the Castoroidinae (*Procastoroides*, *Trogontherium*), the anterio-lateral pointing crista tibiae is more expanded (Schreuder 1929, Shotwell 1970)

In the Staniantsi-beaver this crista tibiae originates at the cranial margin of the proximal tibia and runs distally, terminating close below the middle of the bone. Lateral to this edge a deep carved groove, the fossa lateralis is formed by the anterio-lateral overhang of the crista tibiae. In the most proximal portion of the tibia the fossa lateralis is the deepest. In *Castor* the fossa lateralis starts fading in the proximal one-third of the tibia, in contrast to the Staniantsi-specimens, where the fossa fades at about the middle of the shaft.

The caudal portion of the tibia includes a clear fossa caudalis. In contrast to the fossa lateralis, the extant *C. fiber* shows here a more pronounced expression of this character. In *C. fiber* and in the Staniantsi-beaver the fossa caudalis is deeply carved in the proximal caudal tibia. The fossa

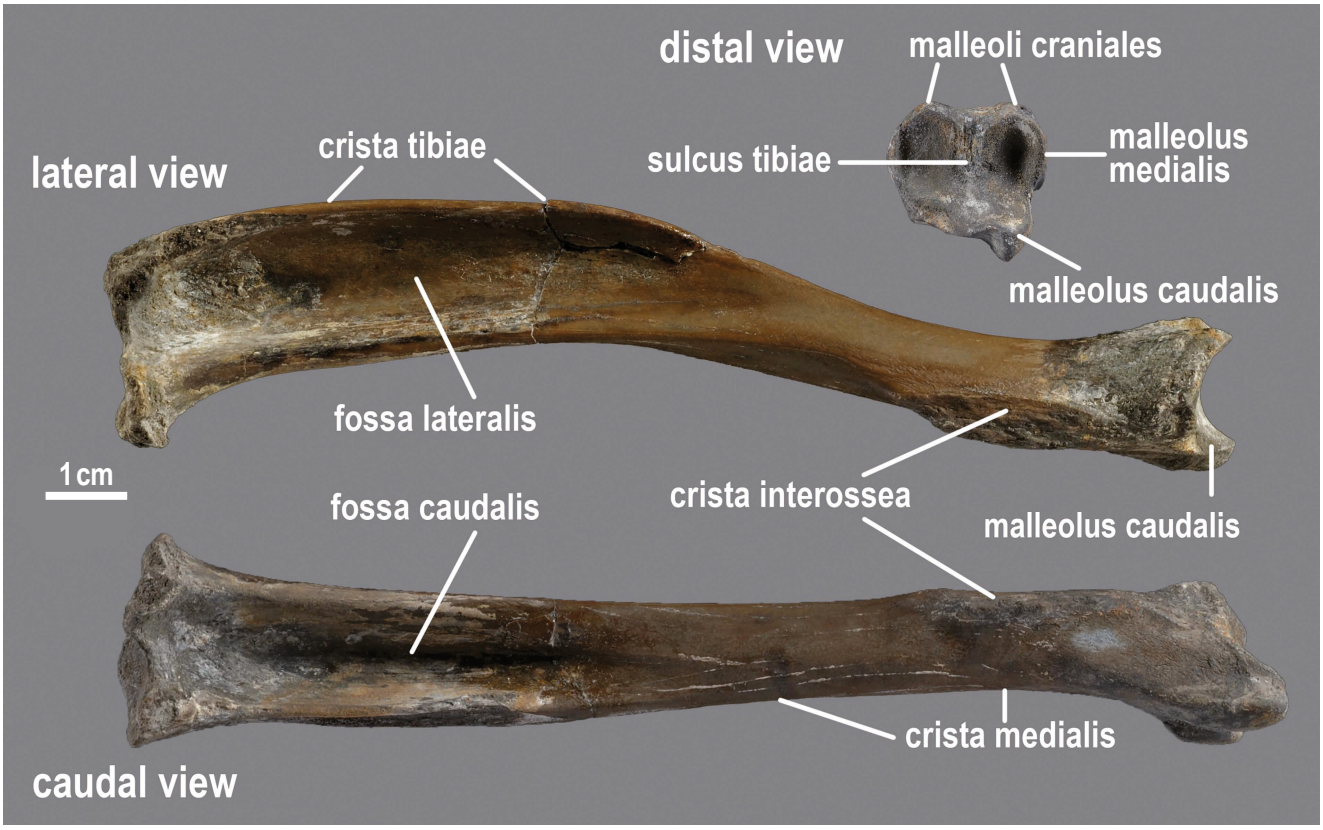

Text-fig. 7. Right tibia of the large Staniantsi-beaver (GPIT/MA/10657) in distal, lateral and caudal view with the illustration of the anatomical terms used for the description of the tibia.

protrudes distally until it fades out at the end of two-thirds in *Castor* and at the middle of the tibia in the Staniantsi-specimens. Two sharp cristae run along the lateral and medial margins of the fossa caudalis. The crista medialis is running medial to the fossa caudalis and the crista interossea is located lateral. The proximal third of the crista medialis and the medial of the crista located area are very tuberous and indicate a large muscle insertion. In the Staniantsi-beaver this tuberosity covers the proximal two-fifths of the crista medialis whereas in the extant *Castor* only one third of this length is reached. In the distal portion of the tibia the crista interossea builds a longitudinal contact surface with the fibula. This tuberosity shows that the fibula is quite firmly fixed with the tibia through soft tissue as cartilage but is not ancylosed. This junction has the length of about one-third of the tibia. In the available extant beaver this junction is about two-fifths of the tibial length and thus longer. The cross section of the distal diaphysis of the tibia is very smooth and rounded. The distal part of the diaphysis and epiphysis are widened in the cranial and medial margin and the distal end is cranio-distally oriented. The distal articulation surface is divided into a medial and a lateral surface by a faint, shallow ridge, running in cranio-caudal direction. In *C. fiber*, both facets are of equal length, while in Castoroidinae the medial facet is elongated cranio-caudally (Shotwell 1970, the text says "lateral facet" but the figure clearly shows an elongated medial facet). The boundary of the fibular side of the distal epiphysis is convex in both the extant *C. fiber* and the Staniantsi-beaver and convex in the Castoroidinae (Schreuder 1929, Shotwell 1970). The distal articular facet of the tibia articulates with the proximal trochlea of the astragalus as a hinge joint. This joint is controlled and directed by different limitations. The distal fibula represents the lateral guidance of the astragalus with the malleolus lateralis. The malleolus medialis at the medial tibia limits the medial margin. Together, these malleoli restrict the medial and lateral sides of the astragalus. The cranial margin of the distal epiphysis of the tibia is dominated by two small cranial malleoli. As an elongation each part of the divided articulation facet terminates in a small cranio-distally pointing malleolus. At the tip of each of these malleoli a tiny additional articulation surface is observable, this is the end-stop of the astragalus, when the foot is maximally dorsi-flexed. A very large malleolus is located at the caudal margin of the distal portion of the tibia (malleolus caudalis). The malleolus caudalis is the caudal extension of the medial half of the articulation facet. Laterally to the malleolus caudalis the sulcus tibiae is located. Additionally, another sulcus runs on the medio-caudal margin of the malleolus caudalis.

Fibula

There is only one small fragment representing a distal fibula without epiphysis (GPIT/MA/03822-4; Pl. 9, Fig. 2). The distal epiphysis of the fibula specimen has fallen off and is lost. The tibia and fibula of this individual were not synostotic fused together. The medial surface of the fragment is very tuberous and fits perfectly to the right tibia GPIT/MA/03822-2. Additionally, all specimens of the GPIT/MA/03822 complex have been found disarticulated together in a small-scale, monospecific bone accumulation and most probably belong to the same individual. The very distal diaphysis of the fibula is triangular in shape. The more proximal but still distal fibula is laterally flattened with a shallow medial ridge forming a flattened triangular cross section with rounded anterior and posterior edges.

Tarsus: Astragalus

Four astragali specimens are available for examination (Pl. 10, Figs 3–5, Pl. 11, Fig. 5). The large and perfectly preserved adult astragalus (GPIT/MA/09796) is used for the main description. Another specimen is, due to taphonomy, heavily compressed. Two smaller juvenile astragali (left and right) were found as part of a larger disarticulated bone accumulation (GPIT/MA/09858-individual). Due to slight damage it is not possible to compare every feature of the latter, but in a combined description of both no feature is missing. These two astragali were also used for the description, especially to identify morphological differences in comparison between juveniles and adults. In contrast to *C. fiber*, the trochlea is not as wide or asymmetrical. The trochlea is concave and transversely grooved with the vertex line running cranio-caudally. This divide is asymmetrical, with the lateral portion occupying nearly two-thirds of the medio-lateral width. In juveniles, this lateral (primary) portion is divided again into two subdivisions, with the lateral subdivision representing two-thirds and the medial one one-third of the lateral (primary) portion. This medial portion is characterised by a convex bead that originates at the proximal margin and is replaced abruptly in the central trochlea by a porous or depth shifted longitudinal area that divides the continuing trochlea in two portions. This central bead is nearly lost in the adult specimen. In contrast to *C. fiber*, where the abrupt distal separation of the trochlea is slightly shifted medially, whereas in the Staniantsi-beaver both parts are more or less in equilibrium. Differing from *C. fiber*, the lateral articulation surface with the fibula (facies articularis malleolaris) is a triangular deep concave facet in the juveniles. In the adult specimens, similar to the extant *C. fiber*, it is slightly convex to planar. The head of the astragalus is very flat and wide, as it is with the extant beaver. Also, very similar to *C. fiber* are the plantar articulation facets (ectal and sustentacular facet) to the calcaneus. These two facets are separated by a sulcus. The ectal facet is nearly as long (proximo-distally) as wide (latero-medially). The shape is approximately triangular. The medial side of this triangle is straight to slightly convex, the proximal side is convex, and the lateral side is sigmoidal with the recession in the proximal half. The distal half of this sigmoid is nearly rectangular in the adult specimen and convex in the juvenile. In *C. fiber* the shape of the ectal facet is variable, being relatively round or triangular, but tends to have equal length and width in common with the Staniantsi-beaver. This is distinct from that of the Castoroidinae (*Procastoroides*, *Dipoides* and *Trogontherium*), which show a typical crescentic and distinctly anteroposteriorly elongated ectal facet (Schreuder 1929, Shotwell 1970). The sustentacular facet runs all the way from the distal, plantar head of the astragalus to the proximal margin, where it represents the plantar surface of a small process. Ginot et al. (2016) recognised this process only in their specimens

belonging to the Castoridae. The articulation facet (facies articularis navicularis) for the navicular bone (Os tarsi centrale) occupies all the distal head of the astragalus and merges medially with the facet of the os tibiale externum. The sustentacular facet and the navicular facet are separated by a groove, often only a small hole-like cavity in the cortical bone in both, *C. fiber* and the Staniantsi-beaver. No such groove is present in the Castoroidinae *Procastoroides* and *Dipoides* (Shotwell 1970). With extant beavers, together with the praecuneiform these bones build a "sixth toe" without a claw, a so called praehallux (see Weber 1927 and Freye 1954). The presence of the distinct articulation facet leaves no doubt about the existence of an os tibiale externus. The presence of a praecuneiform and a two-piece praehallux in the Staniantsi-beaver seems to be most probable, though no such a bone has been found yet.

Tarsus: Calcaneus

There are three specimens representing calcanei (Pl. 9, Fig. 3a–f, Pl. 10, Figs 1, 2). The main description for the calcaneus pertains to a large specimen (GPIT/MA/10658), only lacking the posterior epiphysis where the calcaneal tuberosity is located. Another two fragments consist of a central fragment without distal and proximal characters and a juvenile calcaneus without proximal characters. The latter calcaneus belongs to the juvenile GPIT/MA/09858-individual and articulates perfectly to the corresponding astragalus.

The calcaneus is very elongated in cranio-caudal direction, but not as elongated as *C. fiber*. Additionally, it is stouter and not as slender as in the extant beaver. In dorsal view, the calcaneus is sigmoidal shaped (*C. fiber*: straight), with a laterally pointing proximal margin. The calcaneal process (tuber calcanei) in the fossil specimen is shorter than in *C. fiber*. The calculated calcaneus index (CAI) reaches a value of 0.46 in the Staniantsi-beaver and 0.55 in *C. fiber* (Tab. 1).

There are two proximal articulation facets for the astragalus (ectal facet and sustentacular facet) and also a divided one for the cuboideum (calcaneo-cuboid facet) at the anterior (distal) margin. The ectal facet is slightly concave and longitudinally uniform with a rectangular proximal end. It terminates in an arrow-shaped distal tip, approximately at the central line of the distal calcaneus. In *C. fiber* the facet is more irregular and zigzag-shaped. The ectal facet is separated from the sustentacular facet by a wide, but shallow sulcus. This slightly longitudinally elongated facet is dorsal convex and plantarly projected at the distal end. The caudal margin of the facet is bulge-like bent, tipping also plantarly, forming a saddle-joint. The sustentaculum protrudes far over the medial margin. The sustentaculum of the Castoroidinae *Procastoroides*, *Dipoides* and *Trogontherium* is quite distinct from that of the Castorinae *C. fiber* and the Staniantsi-beaver (Schreuder 1929, Shotwell 1970). In the Castoroidinae the facet is shorter usually approximately rectangular in outline and oriented in parallel to the lateral margin of the calcaneus. Due to the lack of the posterior epiphysis – bearing the tuber calcanei – it can only be assumed, that the insertion of the Achilles tendon has been at least as strongly expressed as in the extant beaver. The anterior margin of the calcaneo-cuboid facet is nearly planar to slightly concave and the placement of the split of the facet is comparable to the one of *C. fiber*. In dorsal view, the dip angle of the facet is orthogonal. This is different from the extant beaver, where a dip angle of approximately 55° is reached.

Tarsus/Metatarsus/Phalanges

The remaining bones from the autopodium are described together (Pl. 1, Fig. 1a–d, Pl. 11, Figs 1–4, 6, Pl. 12, Figs 1–3). There are three of the smaller tarsal bones: one cuboid (os cuboideum), one navicular (os naviculare), and a third cuneiform (lateral cuneiform, os cuneiforme III). Furthermore, the metatarsals consist of fragments of one metatarsal II, one metatarsal III, two metatarsals IV and one metatarsal V. All of these five metatarsals lack the distal end. Neither proximal nor medial phalanges could be identified until now, but there are two distal phalanges (phalanx distalis) of the uncertain digit positions III or IV.

The pedal-skeleton of the large Staniantsi-beaver has many similarities with the extant *Castor*. Although the existing specimens are incomplete, some significant features are visible. The lateral cuneiform (os cuneiforme III, lateral cuneiform) is the largest and therefore dominant bone of the three cuneiformes. Also, the cuboid bone is very dominant in the tarsus. In the castorines the cuboid is medio-laterally narrower with a rectangular outline seen in distal view, whereas in castoroidines, this relation is nearly as wide as high resulting in a nearly square-shaped or slightly rectangular outline (Shotwell 1970). The preserved specimens of the metatarsal II show a similar morphology as the extant *C. fiber* and the Castoroidinae. Metatarsal II is very slender, compared to the dominant metatarsal bones III and IV, that are disproportionally large. The longest and widest metatarsal is the metatarsal IV (GPIT/MA/09859-5), this is typical for all of the Castoridae (Schreuder 1929, Shotwell 1970). Also typical for Castoroidinae and Castorinae is the articulation of the metatarsal V on the proximo-lateral metatarsal IV, without contacting the tarsals (Schreuder 1929, Freye 1954, Shotwell 1970). GPIT/MA/10659, the only metatarsal V, is very well-preserved, lacking only the distal, unfused epiphysis. Comparable to the extant *Castor* the distal end is club-shaped thickened and the epiphysis with adult individuals is still unfused. Similar to *C. fiber*, the metatarsal V is laterally not so much compressed as it is described in the Castoroidinae (Shotwell 1970). Additionally, the *C. fiber* and the Staniantsi-beaver show an elongated and dominant plantar process at the proximal end, that is shifted more distally in the Castoroidinae (see Shotwell 1970: fig. 27). The metatarsal II (GPIT/MA/03822-5) is only lacking the distal third of the bone. The available proximal two-thirds show very similar characteristics to the extant beaver.

There are two large distal phalanges (phalanx distalis) with a very wide and flattened distal tip (GPIT/MA/03889 and GPIT/MA/09951-3). Without any significant asymmetrical features, a declaration of an anatomic placement is not possible. Due to their size and symmetric shape an assignment to digit III or IV can be safely assumed. There are no morphological differences apparent regarding the extant *Castor* in this position.

Discussion

Motion analysis of the forelimb

The forelimb of the large Staniantsi-beaver shares many similarities with the extant *Castor* and also with several fossil castoroidines and castorines. The forelimb is much shorter, in direct comparison to the hindlimb. This fact already demonstrates that the large Staniantsi-beaver, as well as the extant *Castor*, have a huge difference in the functional adaptations of their arms compared to their legs. This directly reflects the fact that beavers are hindlimb-propelled swimmers, and thus have very different fore- and hindlimb proportions (Hinze 1950, Freye 1954, 1978, Dežkin and Safonov 1972, Gingerich 2003, Elissamburu and Vizcaino 2004, Polly 2007, Samuels and Van Valkenburgh 2008). The intermembral index (IM) shows a value of 0.63 in the Staniantsi-beaver. In *C. fiber* (Nawilab/1888) the forelimb is even shorter in relation to the hindlimb (IM = 0.70). In direct comparison of the measurements, the Staniantsi-beaver has a relatively shorter forelimb than the extant *C. fiber* specimen, while the hindlimb reaches similar values. In comparison to several other fossil taxa it is obvious that the Staniantsi-beaver reaches minimum values in castorids (fossil and extant), which implies, that the difference between fore- and hindlimb lengths is particularly high. Samuels and Van Valkenburgh (2008) specify different values for several fossil castorids: *Castoroides ohioensis* (0.82), *Procastoroides sweeti* (0.77), *Dipoides* sp. (0.75), *Castor californicus* (0.74), *Palaeocastor nebrascensis* (0.74) and *Palaeocastor fossor* (0.71). Summarising, the Staniantsi-beaver follows very different functional traits in the forelimb compared to the hindlimb. While the hindlimb is used primarily for the swimming drive in water, the forelimb mainly utilised for digging burrows (Hinze 1950, Freye 1954, Dežkin and Safonov 1972). Taking into consideration that adaptations for swimming and digging in the forelimb of mammals often produce similar results, already the proportional difference to the hindlimb leads to the conclusion, that the far smaller forelimb is not used for propulsion in the swimming process (Gingerich 2003, Elissamburu and Vizcaino 2004, Polly 2007, Samuels and Van Valkenburgh 2008). As it is typical for the high energetic processes of digging (as well as swimming) the muscles have to apply high forces. These forces need to be compensated on and in the bones, which leads to large muscle attachment points on the bones far from the joints and in consequence also to a higher bone compactness (thicker cortical bone, flattening) (Frost 1990a, b, Meier et al. 2013, Ruff et al. 2006). The result is a highly specialised morphology that is a matter of functional anatomy and reflects stronger the ecology of the animal than its phylogeny (Elissamburu and Vizcaino 2003, Samuels and Van Valkenburgh 2008, Meier et al. 2013, Botton-Divet 2016, 2017). The extant members of the genus *Castor* are scratch-diggers (Böker 1935, Hinze 1950, Stein 2000). Following Böker (1935) the anatomy and the motion pattern of the forearm is designed to move excavated (scratched) material to a place below the body, where the foot is able to reach it for the further transport in a backward direction. For this purpose, the muscles need to be optimised in respect to be able to grab digging material with the claws and hand and then to pull this load backwards primarily with the humerus. The morphology of the humerus is dominated by muscle attachment points and origins, which are represented by large extensions and processes. The hand is optimised in size to be a much more powerful "scratcher". With all these commonalities between the extant and extinct beavers and the fossil specimens from Staniantsi, there should now be no doubt, that the forelimb is used in a very similar functional way as the extant *Castor* but probably with a sligthtly smaller forelimb.

The entepicondylar foramen of the humerus

At first sight, the presence of a foramen entepicondylare on one humerus (GPIT/MA/10660) could be of taxonomic relevance. Meanwhile, there are some clues in the literature that suggest this feature relates more to morphological intraspecific variation. To prove this, it is necessary to determine the function of the foramen entepicondylare. Several authors have tried to answer this question. Landry (1958) provides a very comprehensive revision to this issue. Concerning rodents, the foramen entepicondylare can occur in a very variable way. He continues that in extreme cases the foramen can be "… present on one side and absent on the other in the same individual" (Landry 1958: 101). Landry's conclusion comprises that the only testable explanation of that foramens' function in quadrupeds is as a retinaculum – a retaining strap – for the median nerve. Thus, it prevents the nerve from sliding across the elbow joint. In quadrupeds the covering skin of the elbow is slack and does not hold the median nerve securely in place. Sometimes also the brachial artery is enclosed by the foramen. This effect occurs due to the proximity of the nerve and the artery due to a coincidental proximity. The artery does not need any retention because of the anastomoses tying it to the elbow joint. In Landry's opinion there is no disparity between a bony retinaculum and a ligamentous one. He postulates that in many taxa the nerve is just held down by a ligamentous band. These taxa are technically not in possession of a foramen entepicondylare even though this ligament fulfils in every regard the function of a bony one. Especially in rodents, there were some observations of a thin bony bar or alternatively a bony spur (supracondyloid process) that marks the distal root of this ligament taking the same path of the entepicondylar arch. However, the presence of the supracondyloid process in all – except one – of the specimens examined means that there existed a ligamentous arch substituting the bony one in every means of function. Thus, there should be no selective force for or against an ossification of this ligament. Followingly, the ossification of the foramen entepicondylare provides no good criterion that should be used for taxonomic purposes. The presence of the only ossified entepicondylar foramen (GPIT/MA/10660) could be fortuitous and just a matter of intraspecific variability of morphology. In several fossil taxa similar suggestions have been recommended. Rybczynski (2007) shows a huge variability for this character within the different clades of castorids. Filhol (1879) and Schreuder (1928b, 1929) observed the humeri of *Steneofiber viciacensis*, a tiny castorid, from the early Miocene fossil site of Saint Gérand-le-Puy, Allier. They already highlighted that 16 out of 34 available humeral

specimens do have an entepicondylar foramen while the remaining ones do not. Also, Friant (1937) observes the inconsistency of this character. It is quite interesting that in the fossil record the occurrence of the foramen can be more numerous (Schreuder 1928b, 1929, Stirton 1935, Shotwell 1970, Rybczynski 2007). In the modern genus *Castor* this ossified foramen practically never occurs. Also, Freye (1954) does not mention an entepicondylar foramen in his work about the functional anatomy of the beaver-skeleton. Because of his sample-quantity of 15 skeletons (13 Elbe beavers, 1 Norwegian beaver, 1 Rhône beaver) it can be verified that the ossification of the entepicondylar arch in at least the recent Elbe beavers is quite rare. Nevertheless, a ligamentous entepicondylar arch in recent *C. fiber* can be postulated due to the presence of a supracondyloid process that is described by Freye (1954). Subsuming in extant as well as in fossil castorids the presence of at least a ligamentous entepicondylar arch seems plausible and a compelling necessity regarding functional anatomy. Applying the foramen as a primitive amniotic character which is already possessed by most early reptiles (see Romer 1945 and Landry 1958), this feature is more essential in the matter of functional anatomy rather than in a taxonomic relevance.

Motion analysis of the hindlimb

Concerning the elements of the hindlimb it becomes clear, that the large Staniantsi-beaver has various adaptations typical for many semiaquatic rodents like the recent *Castor* and several fossil castorids (Schreuder 1929, Howell 1930, Webb and Blake 1985, Elissamburu and Vizcaino 2004, Samuels and Van Valkenburgh 2008). In general, all elements of the leg show specific insertion points and patterns for muscles and their course. All the bones seem to need special characters to compensate occurring forces while operating in the motion sequence. Especially flattened and thickened bones are typical for many semi-aquatic mammals (Howell 1930, Botton-Divet et al. 2016). In a manner, which is similar to *C. fiber*, the hindlimb is specialised in adaptation to swimming. The autopodial bones compared to the stylo- and zeugopodial bones are remarkably enlarged. Additionally, the femur is strongly flattened and has well-developed processes (trochanter major, minor and tertius). The distal position of the trochanter tertius is directly functionally relevant. The third trochanter is the insertion point of the musculus gluteus maximus and partly for the musculus quadratus femoris and thus plays a distinctive role in the limb retraction during paddling in rodents (Eble 1955). The knee joint is designed in a way that allows rotational movements of the zeugopodium against the stylopodium (femur). Furthermore, the tibia and especially the cranial bending of the distal tibia allow the conclusion that this beaver was not able to extend the knee completely. Instead an angled centre position of the knee can be presumed. With reference to Freye (1954), all of these features describe aquatic adaptations to swimming. Altogether the large Staniantsi-beaver seems to use the hindlimb in a similar way as the extant genus *Castor* does. In addition, the hindlimb is of larger dominance in the Staniantsi-beaver (IM-index 63.01), than it is in the extant *C. fiber* (IM-index 70.40). This means, that the pedal propulsion needs to generate higher forces, than in the extant beaver. This might be necessary due to slight differences in the tail morphology, that do not result in the same additional drive, generated with a very flat and wide tail in the swimming process like in the extant *Castor*. Furthermore, other fossil beavers show even higher IM-indices than *Castor*. Especially the very large fossil beavers (*Trogontherium*, *Procastoroides* and *Castoroides*) have some of the largest IM values (Samuels and Van Valkenburgh 2008). Due to their large body-size those species generate a high profile drag during swimming what makes it necessary to be more specialised to a semiaquatic lifestyle than smaller rodents (Samuels and Van Valkenburgh 2008). This means those large rodents show more dominant, morphological adaptations to, for example, hindlimb-paddling like very large, webbed feet and long hindlimbs.

The foot

Due to the dominance of the two central metapodials, the main forces are focused within a straight-line including digit III and IV (see Freye 1954), the lateral cuneiform (cuneiform III), the cuboid as well as the astragalo-calcaneal complex. Supporting this determination, the metatarsal V does not have any contact to the tarsus and articulates directly with the proximal, latero-plantar margin of the metatarsal IV. Consequently, the forces of the metatarsal V are also directed to the main line of load transfer. The hinge-joint-like articulation is performed below a latero-plantar overhang of the metatarsal IV. This characteristic allows the metatarsal V to cling to and partly disappear below the metatarsal IV when pulled up. Doing the opposite, the digit is laterally braced. This mobility is important for the process of swimming and could indicate a webbed foot because it is necessary to spread the toes during the power stroke to maximise the propulsive force (Webb and Blake 1985). While, the reduction of the pedal size is important to reduce drag during the recovery stroke of the foot (Webb and Blake 1985). The distal phalanges (claws) of the central foot have a very flat and medio-laterally broad tip, which suggests that the keratinous claw sheaths were also broad and blunt. The similarity of the foot of *C. fiber* suggests the functional use would be comparable. The hindlimb primarily is designed as a main drive for swimming (Böker 1935, Freye 1954, 1978, Webb and Blake 1985, Fish 1996, 2000). Additionally, for the scratch-digging, the foot needs to pick up and transport the already loosened sediment to backward through the tunnel (Böker 1935, Hildebrand 1985, Stein 2000). It is obvious that a motion sequence for swimming as well as the transport of sediment in both cases is comparable as both are motions in a dense medium. For this purpose, slender and sharp claws are of course impractical, at least regarding the most powerful digit-positions III and IV.

As already described above, the available fragment of a metatarsal II (GPIT/MA/03822-5) shows very similar characteristics to the extant beaver (Pl. 12, Fig. 2a–f, Text-fig. 8). Additionally, the very slender and subordinate size compared to the other metapodials is very typical for the other fossil castorids (Schreuder 1929, Shotwell 1970). This means there is evidence for the existence of a grooming digit including an implied grooming claw. For several fossil beavers substantiative evidence for the presence of a grooming

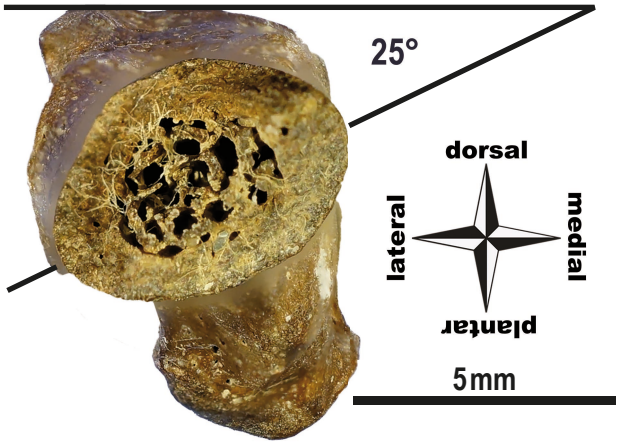

Text-fig. 8. Cross section through the right metatarsal II in distal view. Additionally, the tilt of the greatest shaft diameter compared to the original proximal horizontal orientation is shown.

claw is given. Shotwell (1970) presents grooming claws for several Castoroidinae (*Procastoroides idahoensis*, *Dipoides* sp. and *Monosaulax progressus*). Furthermore, there is also a record for the Castorinae *Steneofiber depereti* (Hugueney and Escuilié 1995). With the extant beaver the neutral position of this finger is characterised by a 45°-rotation and is lifted into a medio-dorsally pointing position.

This twist of the digit already originates in the proximal sector of the metatarsal II. The largest diameter of the diaphysis is enclosed by a lateral and medial crest. While the medial one stays stable on the same level, the lateral crest shifts its location in the distal metatarsus to a rather latero-plantar position. Examining the cross section of the distal diaphysis, the orientation of the largest diameter is tilted by approximately 25° from the horizontal axes (see Text-fig. 8). Consequently, the insertion of the proximal phalanx is already rotated resulting in a medio-dorsally pointing second digit.

The closure of sutures in the appendicular skeleton

In the comparative description of the beaver bones irregularities seem to occur concerning the closure of epiphyseal sutures. Most of those bones with unfused epiphyseal gaps should belong to juvenile individuals (Robertson and Shadle 1954). However, it gets obvious by the comparison of material from extant, confirmed adult beavers, also some of the fossil specimens should belong to adults. Especially with adults, fused, but still suture-bearing epiphyses on some bone positions can be an indicator for a semiaquatic lifestyle (Kükenthal 1891, Freye 1954). As a main pattern it can be recognised that particularly distal epiphyses appear to stay open into a later life stage or not fuse at all. In particular the distal epiphyses of radius and ulna, as well as the femoral and the distal metatarsal epiphysis tend to do so. Especially the flexibility of the distal metatarsus caused by unfused epiphyses is an adaptation probably favourable during the usage of the foot as a paddle in water (Freye 1954). With reference to Kükenthal (1891) this adaptation is sort of a preliminary stage of hyperphalangy as it is often found in aquatic and semiaquatic living vertebrates.

The vertebral column of the tail

Concerning the vertebral column, only caudal vertebra can be discussed.

The presence of large or wing-like (butterfly-shaped) transverse processes on caudal vertebrae indicates a powerful and most probably flattened tail (e.g., Moore 1890, Freye 1954, Shotwell 1970, Hugueney and Escuillié 1995, Daxner-Höck 2004, Rybczynski 2007). In extant beavers the tail is divided into a very muscular furred anterior and a flattened scaly posterior portion (Carlson and Welker 1976, Mahoney and Rosenberg 1981). The anterior vertebrae show elongated transverse processes. The more posteriorly placed vertebrae show a slight dorso-ventral flattening and have expanded, butterfly-shaped transverse processes (Freye 1954, Carlson and Welker 1976, Mahoney and Rosenberg 1981, Rybczynski 2007). Concerning the specimens representing the anterior tail region, it is clearly observable, that there have been very robust and elongated transverse processes. Other caudal vertebrae represent more posterior positions and show several of the features, typical for those in extant castorids. GPIT/MA/09859-3 and GPIT/MA/03851 show butterfly-shaped, expanded transverse processes and due to their size, they can be placed in the posterior portion of the tail. All of those vertebrae show no or only very slightly dorso-ventral flattening. Due to the lack of a fully articulated skeleton or at least a tail or a part of a tail, the exact position of each vertebra cannot be specified with certainty. Nevertheless, this scarce material is already enough to associate the morphological and thus functional features of the vertebrae to the tail region they fit in. This division, in at least two functional portions of the tail, is typical for a semiaquatic adaptation (Freye 1954, Carlson and Welker 1976, Mahoney and Rosenberg 1981). Extant beavers execute a typical pelvic paddling swimming mode (Fish 1993, Allers and Culik 1997). This is a drag-based propulsion mainly with their paddling hindlimbs (Fish 1996, Allers and Culik 1997). Additionally, the tail is used in several movements as an additional propulsion (initiation of a dive), for underwater maneuvers (guiding), for stabilizing postures (bipedal standing or sitting) or for the "warning splash" (Freye 1954, Carlson and Welker 1976). Several extant and fossil species, possessing a flattened tail, provide osteological characters for a comparison of their functional osteology. On one hand there is the Middle Jurassic early mammalian species of *Castorocauda lutrasimilis* (Ji et al. 2006), where a flattened tail might be demonstrated by wide, butterfly-shaped transverse processes, the flattened tail-morphology is also supported by soft-tissue preservation (Ji et al. 2006). Furthermore, the monotreme platypus – *Ornithorhynchus anatinus* Shaw, 1799 – shows considerable transversal processes on the caudal vertebrae and has a well-developed flattened tail (Vogelnest and Allan 2015). On the other hand, the Australian bilby (*Macrotis lagotis*) shows at least in the proximal tail butterfly-shaped transverse processes, possessing a cylindrical tail (Vogelnest and Allan, 2015). Involving functional aspects, bilbies often use the tail as a "third leg" during an upright bipedal set of the body. This results in a certain strain for at least the proximal tail. To compensate this strain, soft tissue has to stabilise it (e.g., muscles, tendons and ligaments), which in turn

needs to have a fundament at the vertebrae – the transverse processes. Consequently, it can be said that having expanded or butterfly-shaped transverse processes on caudal vertebrae means the tail needs to compensate a certain force. During aquatic movements occurring strains are very high and reinforced by a flattened and laterally enlarged tail (Fish 1996, Allers and Culik 1997). Consequently, the adaptations to compensate these forces are enhanced. In general, in beavers the anterior portion of the tail, is bearing enlarged transverse processes, to order, place and guide muscles. The more posterior portion of the tail shapes the flattened tail region and is mostly controlled by the muscles of the anterior portion (Mahoney and Rosenberg 1981). This region is optimised to be as energetic effective as possible (Allers and Culik 1997).

For the large Staniantsi-beaver it can be presumed that it had a flattened tail. For fossil castorids there are several taxa showing distal caudal vertebrae with dorsoventrally compressed and/or laterally expanded transverse processes (Rybczynski 2007). Within the Castoroidinae *Castoroides ohioensis* and *Dipoides tanneri* show both of these characters. The castorine *Steneofiber eseri* only shows expanded transverse processes without a dorsoventral flattening of the vertebrae (Rybczynski 2007). There is a partial skeleton of a castorine from the clay pit of Mataschen (Austria) described with very large transverse processes on the caudal vertebrae indicating a flattened tail (Daxner-Höck 2004). Daxner-Höck (2004) assigned this specimen to *Chalicomys jaegeri* Kaup, 1832 a close relative to *Castor*. Some authors present the theory that *Chalicomys* is the successor of the more primitive genus *Steneofiber* (Stefen 2009, Mörs and Stefen 2010, Stefen 2011). Furthermore, *Chalicomys* is probably the precursor of *Castor* (Stefen 2009). Due to the lack of a dorso-ventral compression in the caudal vertebrae of the Castorinae *Steneofiber eseri*, a cylindrical tail is inferred (Hugueney and Escuillié 1995, Hugueney 1999). The already derived characters in the tail of some Castoroidinae beaver species, that also tend to show a semiaquatic lifestyle and possibly flattened tail, show that this adaptation probably emerged several times in castorids and thus evolved maximum adaptations separately in Castorinae and Castoroidinae (see tail character states in Rybczynski 2007).

Conclusion

The postcranial skeleton of beavers is rarely used as a key aspect in scientific research. The present work demonstrates that every little component of the skeleton has an own imprint of information about the functional anatomy. Nearly every bone can be used to get piece by piece an overall picture of the motion sequences and finally the locomotor behaviour of the whole animal.

For the large Staniantsi-beaver it can be concluded that a semiaquatic lifestyle comparable to extant beavers seems to be the most appropriate. Especially the forelimb shows features for a scratch-digging behaviour that is supported by a hindlimb with the ability of further transporting the excavated material. Furthermore, the large Staniantsi-beaver has many more features in common with the extant *Castor*. There is a hindlimb with the typical adaptations for paddling and a forelimb with a dominant fossorial modification. Moreover, the caudal vertebrae indicate a flattened tail that could have been used in a similar way as in recent castorids do. Lastly, the large Staniantsi-beaver fits perfectly into the suggested ecosystem of the Staniantsi-Mazgoš basin during the uppermost Miocene with a mostly swampy to lacustrine environment and seems to be an ecological equivalent to the extant beaver. Concerning postcranial characters, the large Staniantsi-beaver belongs to the Castorinae beaver clade and could be placed within the genus *Castor* or *Chalicomys*. To consolidate this assumption the available numerous cranial and dental elements have to be included, too. These elements carry the current defining characters of the most rodent taxa. But especially in fossil beavers it is necessary to include postcranial characters in the taxonomic definitions to expand and strengthen phylogenetic approaches. Thus, it may be possible to clarify the systematic position of taxa with poor records in cranial material. For fossil beavers the genus *Chalicomys* (*Palaeomys*) is one of the best examples. This genus still doesn't appear in the recent study by Rybczynski (2007) providing phylogenetic approaches for the Castoridae. According to different authors this genus should be an essential component of the fossil lineage possibly proceeding from *Steneofiber* over *Chalicomys* (*Palaeomys*) to the extant genus *Castor* (Stefen 2009). The reason for Rybczynski (2007) not including *Chalicomys* in the analysis is that, so far, no complete skull of *Chalicomys* is available. The Staniantsi fossil site could play a key role in respect to these taxonomic and phylogenetic issues. In addition to the described postcranial elements a large number of dental and bony cranial (mandibles) specimens are available and can be used to place the large Staniantsi-beaver in a taxonomic framework. Fossil rodent taxonomy is dominated by cranial features and it cannot be denied that in many fossil accumulations cranial elements, in particular teeth, have the best opportunity to be preserved. However, in many cases it is simply impossible to attribute postcranial material to taxa that have been described based on craniodental remains without the availability of complete skeletons. Many more postcranial studies are needed to supplement phylogenetic, taxonomic and ecological approaches in rodents and especially beavers.

Acknowledgements

We want to acknowledge all members of the diverse research trips to Bulgaria that detected and collected the presented material and much more still untreated specimens. We would also like to express our gratitude to Ilona Gold, Felix Augustin and Panagiotis Kampouridis for discussions and improvement of the manuscript. Further, we want to thank the Nawilab, namely Wolfgang Lechner, for providing osteological reference material. We also want to acknowledge Henrik Stöhr for his great job in the preparation of the challenging Staniantsi fossils. Finally, we would like to thank the editor Thomas Lehmann, as well as the reviewers Clara Stefen and Joshua Samuels for their helpful comments and suggestions on the manuscript.

References

Allers, D., Culik, B. M. (1997): Energy Requirements of Beavers (*Castor canadensis*) Swimming Underwater. – Physiological Zoology, 70(4): 456–463. https://doi.org/10.1086/515852

Angelov, V., Haydutov, I., Dimitrova, R., Yanev, S., Tronkov, D., Sapunov, I., Chumachenko, P., Nikolov, T., Chunev, D., Tzankov, T. (1993): Geological Map of Bulgaria, scale 1:100.000, sheet Pirot. – Committee of Geology and Mineral Resources, Sofia.

Böker, H. (1935): Einführung in die vergleichende biologische Anatomie der Wirbeltiere. – Gustav Fischer, Jena, 228 pp.

Botton-Divet, L., Cornette, R., Fabre, A. C., Herrel, A., Houssaye, A. (2016): Morphological analysis of long bones in semi-aquatic mustelids and their terrestrial relatives. – Integrative and comparative biology, 56(6): 1298–1309. https://doi.org/10.1093/icb/icw124

Botton-Divet, L., Cornette, R., Houssaye, A., Fabre, A.-C., Herrel, A. (2017): Swimming and running: A study of convergence in long bone morphology among semi-aquatic mustelids (Carnivora: Mustelidae). – Biological Journal of the Linnean Society, 121(1): 1–12. https://doi.org/10.1093/biolinnean/blw027

Carlson, M., Welker, W. I. (1976): Some Morphological, Physiological and Behavioral Specializations in North American Beavers (Castor canadensis). – Brain, Behavior and Evolution, 13: 302–326. https://doi.org/10.1159/000123818

Casanovas-Vilar, I., Alba, D. M. (2011): The Never-Ending Problem of Miocene Beaver Taxonomy. – Acta Palaeontologica Polonica, 56: 217–220. https://doi.org/10.4202/app.2010.0051

Daxner-Höck, G. (2004): Biber und ein Zwerghamster aus Mataschen (Unter-Pannonium, Steirisches Becken). – Joannea, Geologie und Paläontologie, 5: 19–33.

Dežkin, V. V., Safonov, V. G. (1972): Die Biber der alten und neuen Welt. – A. Ziemsen Verlag, Wittenberg Lutherstadt, 172 pp.

Driesch, A. von den (1976): A guide to the measurement of animal bones from archaeological sites: as developed by the Institut für Palaeoanatomie, Domestikationsforschung und Geschichte der Tiermedizin of the University of Munich. – Peabody Museum bulletin, 1: i–ix + 1–136.

Eble, H. (1955): Funktionelle Anatomie der Extremitäten-muskulatur von *Ondatra zibethica*, Beiträge zur funktionellen Anatomie der Bisamratte (II.). – Wissenschaftliche Zeitschrift der Martin-Luther-Universität, Halle-Wittenberg, Mathematisch-Natur-wissenschaftliche Reihe, 4(5): 977–1004.

Elissamburu, A., Vizcaino, S. F. (2004): Limb proportions and adaptations in caviomorph rodents (Rodentia: Caviomorpha). – Journal of Zoology, 262(2): 145–159. https://doi.org/10.1017/S0952836903004485

Felten, H., Helfricht, A., Storch, G. (1973): Die Bestimmung der europäischen Fledermäuse nach der distalen Epiphyse des Humerus. – Senckenbergiana biologica, 54: 291–297.

Fejfar, O., Storch, G. (1994): Das Nagetier von Valeč – Waltsch in Böhmen – ein historischer fossiler Säugetierfund (Rodentia: Myoxidae). – Münchner Geowissenschaftliche Abhandlungen, Reihe A Geologie und Paläontologie, 26: 5–34.

Filhol, H. (1879): Etudes des Mammifères fossiles de Saint-Gérand-le-Puy (Allier). – Annales des sciences geologiques, 10(3): 1–251, 30 pls.

Fish, F. E. (1993): Influence of hydrodynamic design and propulsive mode on mammalian swimming energetics. – Australian Journal of Zoology, 42: 79–101. https://doi.org/10.1071/ZO9940079

Fish, F. E. (1996): Transitions from Drag-based to Lift-based Propulsion in Mammalian Swimming. – American Zoologist, 36: 628–641. https://doi.org/10.1093/icb/36.6.628

Fish, F. E. (2000): Biomechanics and Energetics in Aquatic and Semiaquatic Mammals: Platypus to Whale. – Physiological and Biochemical Zoology 73(6): 683–698. https://doi.org/10.1086/318108

Freye, H.-A. (1954): Beiträge zur funktionellen Anatomie des Biberskelettes. – Wissenschaftliche Zeitschrift der Martin-Luther-Universität, Halle-Wittenberg, Mathe-matisch-Naturwissenschaftliche Reihe, 3(5): 1101–1136.

Freye, H.-A. (1978): *Castor fiber* Linnaeus, 1758 – Europäischer Biber. – In: Niethammer, J., Krapp, F. (eds), Handbuch der Säugetiere Europas 1: Rodentia: 1 (Sciuridae, Castoridae, Gliridae, Muridae). Aula-Verlag, Wiesbaden, pp. 184–200.

Friant, M. (1937): Recherches sur Les Caractères Ostéologiques des Castoridés (Steneofiber, Castor). – Archives du Muséum d'Histoire Naturelle, Paris, 6: 106–124.

Frost, H. M. (1990a): Skeletal structural adaptations to mechanical usage (SATMU): 1. Redefining Wolff's Law: The bone modelling problem. – The Anatomical Record, 226: 403–413. https://doi.org/10.1002/ar.1092260402

Frost, H. M. (1990b): Skeletal structural adaptations to mechanical usage (SATMU): 2. Redefining Wolff's Law: The remodelling problem. – The Anatomical Record, 226: 414–422. https://doi.org/10.1002/ar.1092260403

Gervais, P. (1869): Zoologie et Palaeontologie générales. 1re série avec atlas. – Arthus Bertrand, libraire-éditeur, Paris, vii + 263 pp., 50 pls.

Gingerich, P. D. (2003): Land-to-sea transition in early whales: evolution of Eocene Archaeoceti (Cetacea) in relation to skeletal proportions and locomotion of living semiaquatic mammals. – Paleobiology, 29: 429–454. https://doi.org/10.1666/0094-8373(2003)029<0429:LTIEWE>2.0.CO;2

Ginot, S., Hautier, L., Marivaux, L., Vianey-Liaud, M. (2016): Ecomorphological analysis of the astragalo-calcaneal complex in rodents and inferences of locomotor behaviours in extinct rodent species. – PeerJ, 4: e2393 (49 pp.). https://doi.org/10.7717/peerj.2393

Habersetzer, J., Storch, G. (1987): Klassifikation und funktionelle Flügelmorphologie paläogener Fledermäuse (Mammalia, Chiroptera). – Courier Forschungsinstitut Senckenberg, 91: 117–150.

Hemprich, W. (1820): Grundriss der Naturgeschichte für höhere Lehranstalten. – August Rücker, Berlin, 29 pp.

Hildebrand, M., Bramble, D. M., Liem, K. F., Wake, D. B. (eds) (1985): Functional Vertebrate Morphology. – Belknap Press, Harvard, 430 pp.

Hinze, G. (1950): Der Biber – Körperbau und Lebensweise, Verbreitung und Geschichte. – Akademie-Verlag, Berlin, 216 pp.

Howell, A. B. (1930): Aquatic mammals: Their adaptations to life in water. – Charles C. Thomas, Springfield, Illinois, 338 pp.

Hugueney, M. (1999): Family Castoridae. – In: Rössner, G. E., Heissig, K. (eds), The Miocene Land Mammals of Europe. Verlag Dr. Friedrich Pfeil, München, pp. 281–300.

Hugueney, M., Escuillié, F. (1995): K-strategy and adaptative specialization in *Steneofiber* from Montaigu-le-Blin (dept. Allier, France; Lower Miocene, MN 2a, ± 23 Ma): first evidence of fossil life-history strategies in castorid rodents. – Palaeogeography. Palaeoclimatology, Palaeoecology, 113(2-4): 217–225. https://doi.org/10.1016/0031-0182(95)00050-V

Ji, Q., Luo, Z.-X., Yuan, C.-X., Tabrum, A. R. (2006): A Swimming Mammaliaform from the Middle Jurassic and Ecomorphological Diversification of Early Mammals. – Science 311: 1123–1127. https://doi.org/10.1126/science.1123026

Konjarov, G. (1932): Die Braunkohlen Bulgariens. – Pernik [Publishing House of the National Coal Mine], Sofia, 303 pp., 75 pls. (in Bulgarian with German summary)

Korth, W.W. (2002): Comments on the Systematics and Classification of the Beavers (Rodentia, Castoridae). – Journal of Mammalian Evolution, 8: 279–296. https://doi.org/10.1023/A:1014468732231

Kükenthal, W. (1891): Über die Anpassung von Säugethieren an das Leben im Wasser. –Zoologische Jahrbücher, Abtheilung für Systematik, Geographie und Biologie der Thiere, 5: 373–399.

Landry, S. O. (1958): The Function of the Entepicondylar Foramen in Mammals. – American Midland Naturalist, 60(1): 100–112. https://doi.org/10.2307/2422468

Linnaeus, C. (1758): Systema naturae Per Regna Tria Naturae, Secundum Classes, Ordines, Genera, Species cum Characteribus, Differentiis, Synonymis, Locis. – Laurentius Salvius, Holmiae [Stockholm], 824 pp. https://doi.org/10.5962/bhl.title.542

Mahoney, J. M., Rosenberg, H. I. (1981): Anatomy of the tail in the beaver (*Castor canadensis*). – Canadian Journal of Zoology, 59: 390–399. https://doi.org/10.1139/z81-057

Meier, P. S., Bickelmann, C., Scheyer, T. M., Koyabu, D., Sánchez-Villagra, M. R. (2013): Evolution of bone compactness in extant and extinct moles (Talpidae): exploring humeral microstructure in small fossorial mammals. – BMC Evolutionary Biology, 13: 55 (10 pp.). https://doi.org/10.1186/1471-2148-13-55

Mol, D., de Vos, J. (1995): Een dijbeen van een uitgestorven bever, *Trogontherium cuvieri* Fischer (1809), van de Noordzeebodem en enkele wetenswaardigheden over deze bever [A femur of an extinct beaver, *Trogontherium cuvieri* Fischer (1809), from the North Sea bed and some things worth knowing about this beaver] – Grondboor en Hamer, 2: 29–37. (in Dutch)

Moore, J. (1890): Concerning a skeleton of the great fossil beaver, *Castoroides ohioensis*. – Journal of the Cincinnati Society of Natural History, 13: 138–169.

Mörs, T., Stefen, C. (2010): The Castorid *Steneofiber* from NW Germany and Its Implications for the Taxonomy of Miocene Beavers. – Acta Palaeontologica Polonica, 55: 189–198. https://doi.org/10.4202/app.2009.0013

Polly, P. D. (2007): Limbs in mammalian evolution. – In: Hall, B. K. (ed.), Fins into Limbs: Evolution, Development, and Transformation. University of Chicago Press, Chicago, pp. 245–268.

Robertson, R. A., Shadle, A. R. (1954): Osteologic criteria of age in beavers. – Journal of Mammalogy, 35(2): 197–203. https://doi.org/10.2307/1376033

Romer, A. S. (1945): Vertebrate Paleontology. – University of Chicago Press, Chicago, 687 pp.

Ruff, C., Holt, B., Trinkaus, E. (2006): Who's afraid of the big bad Wolff?: "Wolff's law" and bone functional adaptation. – American Journal of Physical Anthropology, 129: 484–498. https://doi.org/10.1002/ajpa.20371

Rybczynski, N. (2007): Castorid Phylogenetics: Implications for the Evolution of Swimming and Tree-Exploitation in Beavers. – Journal of Mammalian Evolution, 14: 1–35. https://doi.org/10.1007/s10914-006-9017-3

Samuels, J. X., Van Valkenburgh, B. (2008): Skeletal Indicators of Locomotor Adaptations in Living and Extinct Rodents. – Journal of Morphology, 269: 1387–1411. https://doi.org/10.1002/jmor.10662

Schaller, O. (ed.) (2007): Illustrated veterinary anatomical nomenclature (2nd ed). – Enke, Stuttgart, 614 pp.

Schmidt-Kittler, N., Storch, G. (1985): Ein vollständiges Theridomyiden-Skelett (Mammalia: Rodentia) mit Rennmaus-Anpassungen aus dem Oligozän von Céreste, S-Frankreich. – Senckenbergiana lethaea, 66: 89–109.

Schreuder, A. (1928a): *Castor praefiber* Depéret in der Fauna von Roussillion. – Paläontologische Zeitschrift, 9: 374–378. https://doi.org/10.1007/BF03041563

Schreuder, A. (1928b): Humerus von *Steneofiber depereti* Mayet. – Paläontologische Zeitschrift, 10: 125–129. https://doi.org/10.1007/BF03041567

Schreuder, A. (1929): *Conodontes* (*Trogontherium*) and *Castor* from the Teglian clay compared with the Castoridae from other localities. – Archives du Musee' Teyler, 3: 99–320.

Shotwell, J. A. (1970): Pliocene mammals of southeast Oregon and adjacent Idaho. – Bulletin of the Museum of Natural History, University of Oregon, 17: 1–103.

Stefen, C. (1997): *Steneofiber eseri* (Castoridae, Mammalia) von der Westtangente bei Ulm im Vergleich zu anderen Biberpopulationen. – Stuttgarter Beiträge zur Naturkunde, Serie B (Geologie und Paläontologie), 255: 1–73.

Stefen, C. (2009): The European Tertiary beaver *Chalicomys jaegeri* (Rodentia: Castoridae) revisited. – Kaupia – Darmstädter Beiträge zur Naturgeschichte, 16: 161–174.

Stefen, C. (2011): A Brief Overview of the Evolution of European Tertiary Beavers. – Baltic Forestry, 17(1): 148–153.

Stein, B. R. (2000): Morphology of subterranean rodents. – In: Lacey, E. A., Patton, J. L., Cameron, G. N. (eds), Life Underground: The Biology of Subterranean Rodents. University of Chicago Press, Chicago, Illinois, pp. 19–61.

Stirton, R. A. (1936): A review of tertiary beavers. – University of California Publications in Geological Sciences, 23(13): 391–458. https://doi.org/10.1144/transed.13.3.391

Storch, G., Engesser, B., Wuttke, M. (1996): Oldest fossil record of gliding in rodents. – Nature, 379: 439–441. https://doi.org/10.1038/379439a0

Uhl, D., Dolezych, M., Böhme, M. (2014): *Taxodioxylon*-like charcoal from the Late Miocene of western Bulgaria. – Acta Palaeobotanica, 54: 101–111. https://doi.org/10.2478/acpa-2014-0004

Utescher, T., Ivanov, D., Harzhauser, M., Bozukov, V., Ashraf, A. R., Rolf, C., Urbat, M., Mosbrugger, V. (2009): Cyclic climate and vegetation change in the late Miocene of Western Bulgaria. – Palaeogeography, Palaeoclimatology, Palaeoecology, 272: 99–114. https://doi.org/10.1016/j.palaeo.2008.11.014

Vogelnest, L., Allan, G. (2015): Radiology of Australian mammals. – CSIRO Publishing, Clayton South, 307 pp. https://doi.org/10.1071/9780643108653

Webb, P. W., Blake, R. W. (1985): Swimming. – In: Hildebrand, M., Bramble, D. M., Liem, K. F., Wake, D. B. (eds), Functional Vertebrate Morphology. Belknap Press, Harvard, pp. 111–128.

Weber, M. (1927): Die Säugetiere – Einführung in die Anatomie und Systematik der recenten und fossilen Mammalia, Band I: Anatomischer Teil, Die Säugetiere (2nd ed). – Gustav Fischer, Jena, 444 pp.

Explanations to the plates

PLATE 1

Postcranial material of the large Staniantsi-beaver – vertebrae and one metatarsal bone

1. Right os metatarsale IV (GPIT/MA/03859-5); a – distal, b – medial, c – lateral, d – proximal view.
2. Proximal vertebra caudalis (GPIT/MA/09859-4); a – cranial (axial), b – dorsal, c – ventral, d – caudal (axial), e – lateral (sinistral) view.
3. Proximal vertebra caudalis (GPIT/MA/03822-7); a – dorsal, b – ventral, c – axial view.
4. Medial vertebra caudalis (GPIT/MA/09859-3); a – ventral, b – cranial (axial), c – dorsal view.
5. Proximal vertebra caudalis (GPIT/MA/09409); a – cranial (axial), b – caudal (axial), c – lateral (dextral), d – dorsal, e – ventral view.
6. Proximal vertebra caudalis (GPIT/MA/09824); a – axial, b – axial, c – lateral, d – dorsal, e – ventral view.
7. Distal caudal vertebrae (GPIT/MA/03851); a – cranial (axial), b – caudal (axial), c – lateral (sinistral), d – dorsa, e – ventral view.
8. Distal vertebra caudalis (GPIT/MA/03893); a – cranial (axial), b – caudal (axial), c – lateral (sinistral), d – dorsal, e – ventral view.

Note the different scale bars in (7) and (8), all other specimens are on the same scale.

PLATE 2

Postcranial material of the large Staniantsi-beaver – forelimb: radius and scapula

1. Right radius (GPIT/MA/03822-3); a – lateral, b – caudal, c – cranial, d – medial, e – proximal view (left margin pointing medially, top facing cranially).
2. Right radius in proximal view (GPIT/MA/09858-3); same orientation as Fig. 1e.
3. Left scapula (GPIT/MA/03819); a – lateral, b – distal view.
4. Right scapula (GPIT/MA/09858-9); a – cranial, b – distal, c – lateral, d. caudal view.

All specimens on the same scale.

PLATE 3

Postcranial material of the large Staniantsi-beaver – forelimb: humerus

1. Left humerus (GPIT/MA/09931); a – lateral, b – cranial, c – caudal, d – medial, e – distal view.
2. Right humerus (GPIT/MA/09793); a – cranial, b – caudal view.
3. Right humerus distal end (GPIT/MA/09933); a – cranial, b – caudal view.

All specimens on the same scale.

PLATE 4

Postcranial material of the large Staniantsi-beaver – forelimb: humerus

1. Right humerus (GPIT/MA/10660); a – caudal, b – cranio-medial, c – cranio-lateral, d – distal, e – proximal view.
2. Right humerus (GPIT/MA/09935); a – caudal, b – distal, c – proximal, d – cranial view.

All specimens on the same scale.

PLATE 5

Postcranial material of the large Staniantsi-beaver – forelimb: ulna

1. Left ulna (GPIT/MA/03758); a – lateral, b – cranial, c – medial view.
2. Left ulna (GPIT/MA/09968); a – cranial, b – lateral view.
3. Right ulna (GPIT/MA/09743); a – lateral, b – cranial view.
4. Left ulna (GPIT/MA/09468); a – lateral, b – cranial, c – medial view.

All specimens on the same scale.

PLATE 6

Postcranial material of the large Staniantsi-beaver – hindlimb: pelvis and femur

1. Right innominate bone (GPIT/MA/09393); a – medial, b – lateral (right end pointing cranially), c – dorsal view.
2. Right femur (GPIT/MA/09934); a – distal, b – proximal, c – cranial, d – medial, e – lateral, f – caudal view.

All specimens on the same scale.

PLATE 7

Postcranial material of the large Staniantsi-beaver – hindlimb: femur

1. Right femur (GPIT/MA/9755); cranial view.
2. Right femur (GPIT/MA/09963); cranial view.
3. Right femur (GPIT/MA/09858-6); a – cranial, b – caudal, c – lateral view.
4. Left femur juvenile specimen (GPIT/MA/03882); a – caudal, b – cranial view.

All specimens on the same scale.

PLATE 8

Postcranial material of the large Staniantsi-beaver – hindlimb: tibia

1. Right tibia (GPIT/MA/10657); a – caudal, b – cranial, c – lateral, d – distal, e – proximal view (epiphysis is missing).
2. Right tibia (GPIT/MA/09765); a – caudal, b – cranial view, c – cross-section of proximal shaft, d – distal, e – lateral, f – medial view.
3. Right tibia (GPIT/MA/03822-2); a – cranial, b – lateral, c – distal view.
4. Right tibia proximal articulation facet (GPIT/MA/09767); a – lateral, b – distal, c – proximal view.

All specimens on the same scale.

PLATE 9

Postcranial material of the large Staniantsi-beaver – hindlimb: tibia, fibula and calcaneus

1. Left tibia (adult) (GPIT/MA/09861); a – lateral, b – cranial, c – medial view.
2. Right fibula (subadult) (GPIT/MA/03822-4); a – medial, b – lateral, c – cranial, d – caudal, e – distal view, f – cross-section of distal shaft.
3. Left calcaneus (adult) (GPIT/MA/10658); a – medial, b – lateral, c – plantar, d – dorsal, e – distal, f – proximal view (epiphysis missing).

Note the different scale bars.

PLATE 10

Postcranial material of the large Staniantsi-beaver – hindlimb: calcaneus and astragalus

1. Right calcaneus (GPIT/MA/3922); a – dorsal, b – lateral, c – medial, d – proximal, e – distal view.
2. Left calcaneus (GPIT/MA/09858-5); a – distal, b – proximal, c – dorsal, d – plantar, e – medial view.
3. Left astragalus (GPIT/MA/09796); a – distal, b – proximal, c – dorsal, d – plantar, e – medial, f – lateral view.
4. Left astragalus (GPIT/MA/09858-1); a – distal, b – proximal, c – dorsal, d – plantar, e – lateral, f – medial view.
5. Right astragalus (GPIT/MA/09858-2); a – proximal, b – distal, c – plantar, d – dorsal, e – medial, f – lateral view.

All specimens on the same scale.

PLATE 11

Postcranial material of the large Staniantsi-beaver – hindlimb: autopodium of the GPIT/MA/09858-individual

1. Left os metatarsale III (GPIT/MA/09858-14); a – proximal view, b – distal view of cross-section through the shaft, c – lateral, d – medial, e – plantar, f – dorsal view.
2. Left os metatarsale IV (GPIT/MA/09858-13); a – distal, b – lateral, c – plantar, d – dorsal view.
3. Left os cuneiforme III (GPIT/MA/09858-12); a – proximal, b – distal, c – medial, d – plantar, e – dorsal view.
4. Left os naviculare (GPIT/MA/09858-11); a – distal, b – medial, c – proximal, d – plantar, e – dorsal view.
5. Left astragalus (GPIT/MA/09858-1); dorsal view.
6. Left os cuboideum (GPIT/MA/09858-10); a – proximal, b – distal, c – medial, d – dorsal, e – plantar view.

All specimens on the same scale.

PLATE 12

Postcranial material of the large Staniantsi-beaver – hindlimb: autopodium and one phalanx distalis from the forelimb

1. Right os metatarsale V (GPIT/MA/10659); a – dorsal, b – lateral, c – proximal, d – medial, e – plantar view.
2. Right os metatarsale II (GPIT/MA/03822-5); a – dorsal, b – lateral, c – proximal, d –medial, e – plantar view, f – cross-section through the shaft in distal view.
3. Pedal phalanx distalis of digit III or IV (GPIT/MA/03889); a – lateral (sinistral), b – plantar, c – proximal, d – distal, e – lateral (dextral), f – dorsal view.
4. Manual phalanx distalis (GPIT/MA/03841) (unknown digit position); a – dorsal, b – palmar, c – lateral, d – lateral, e – proximal view.

All specimens on the same scale.

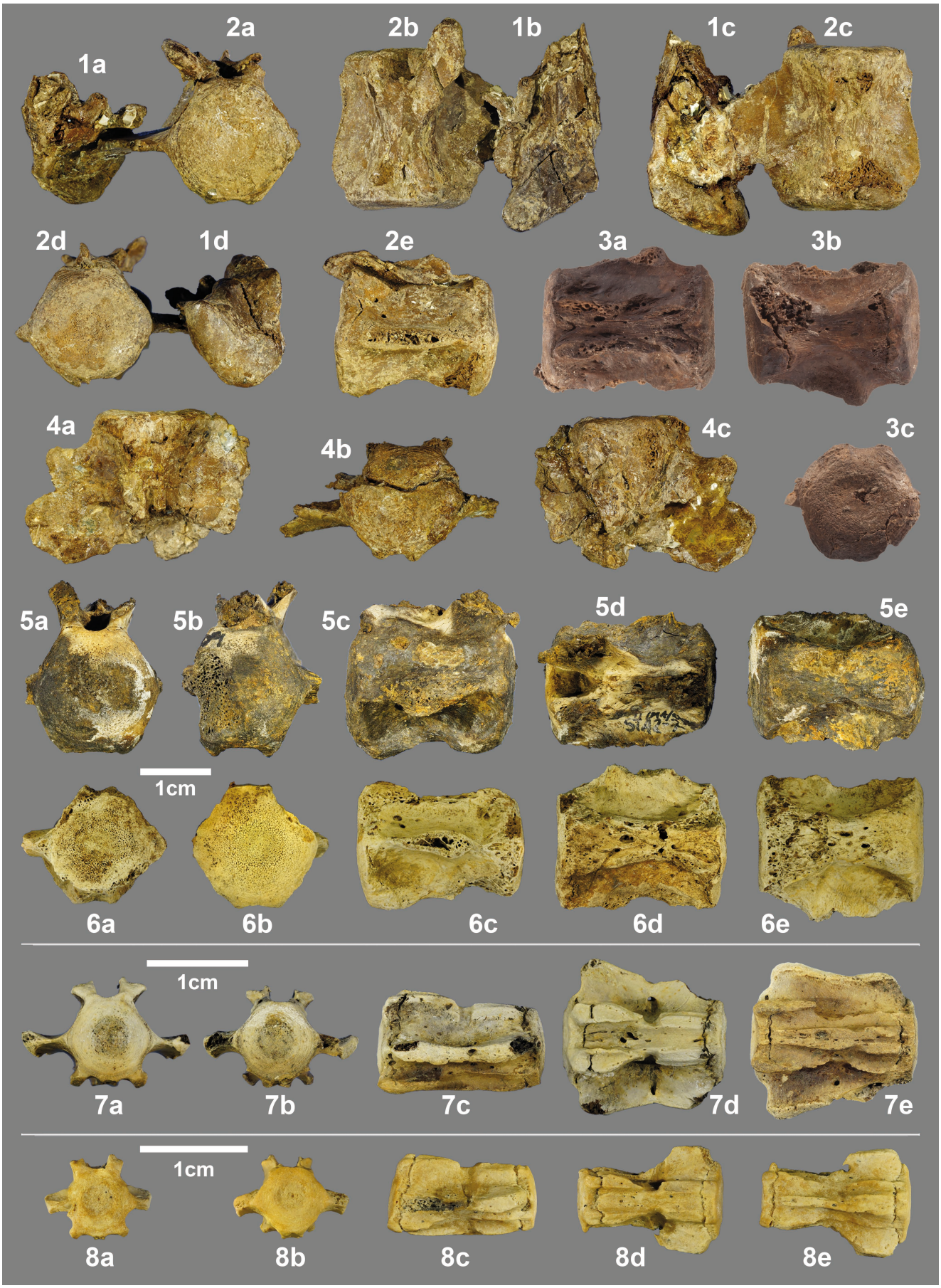
1a
2a
2b
1b
1c
2c
2d
1d
2e
3a
3b
4a
4b
4c
3c
5a
5b
5c
5d
5e
1cm
6a
6b
6c
6d
6e
1cm
7a
7b
7c
7d
7e
1cm
8a
8b
8c
8d
8e

PLATE 2


1a
1b
1c
1d
1e
2a
2b
3a
3b
1cm

PLATE 4

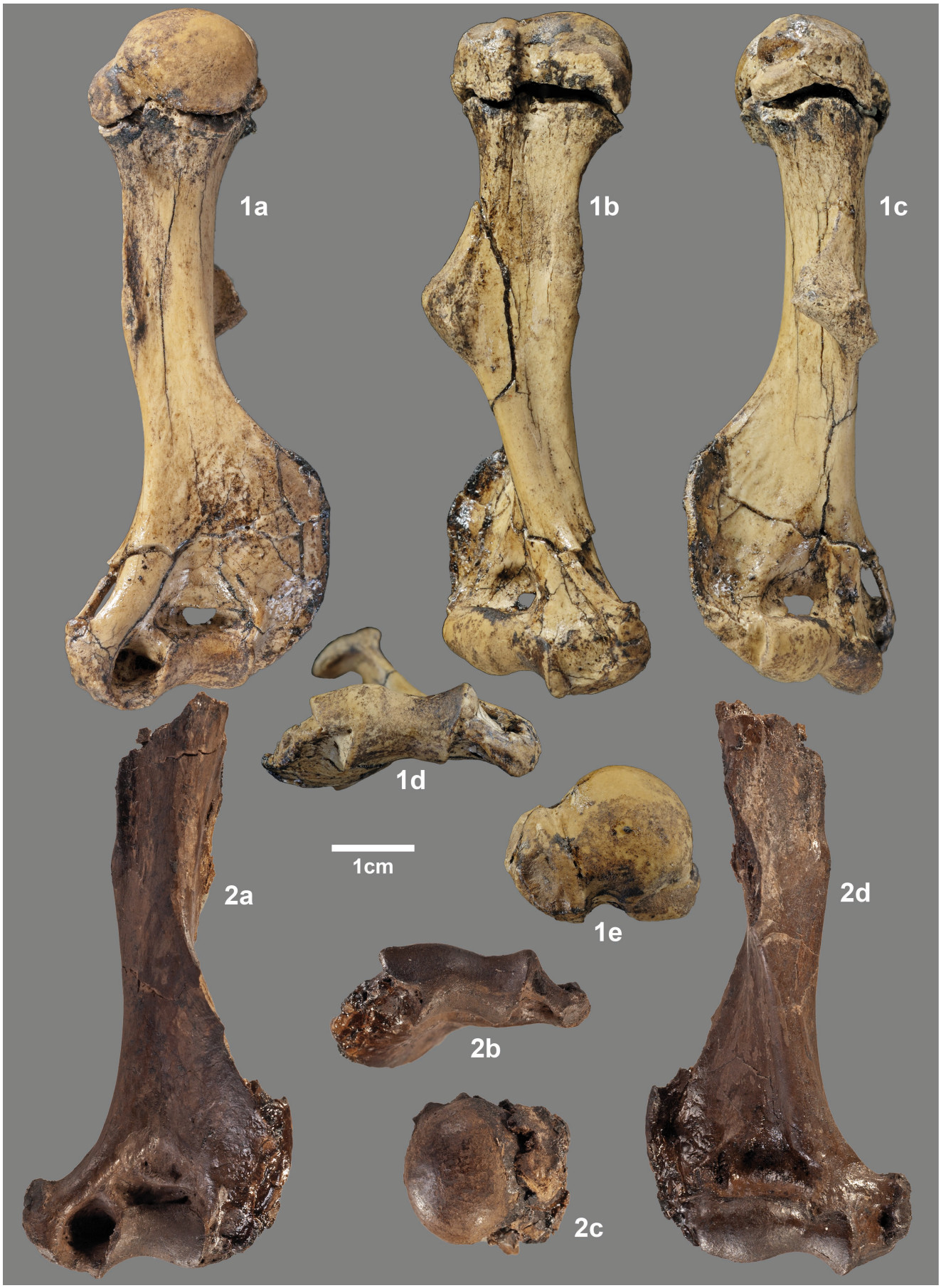


1a
1b
1c
1cm
2a
2b
3a
3b
4a
4b
4c

PLATE 6

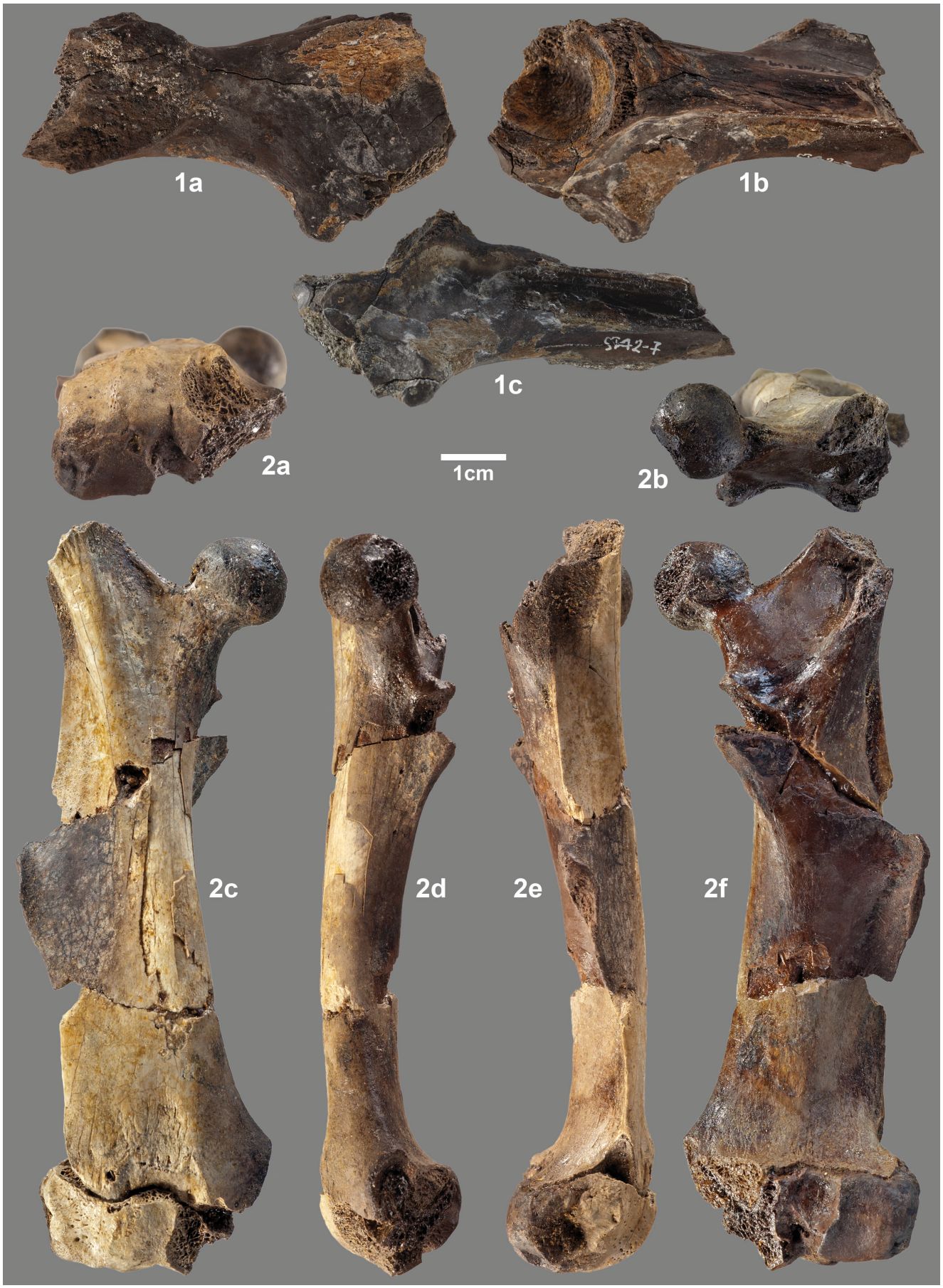

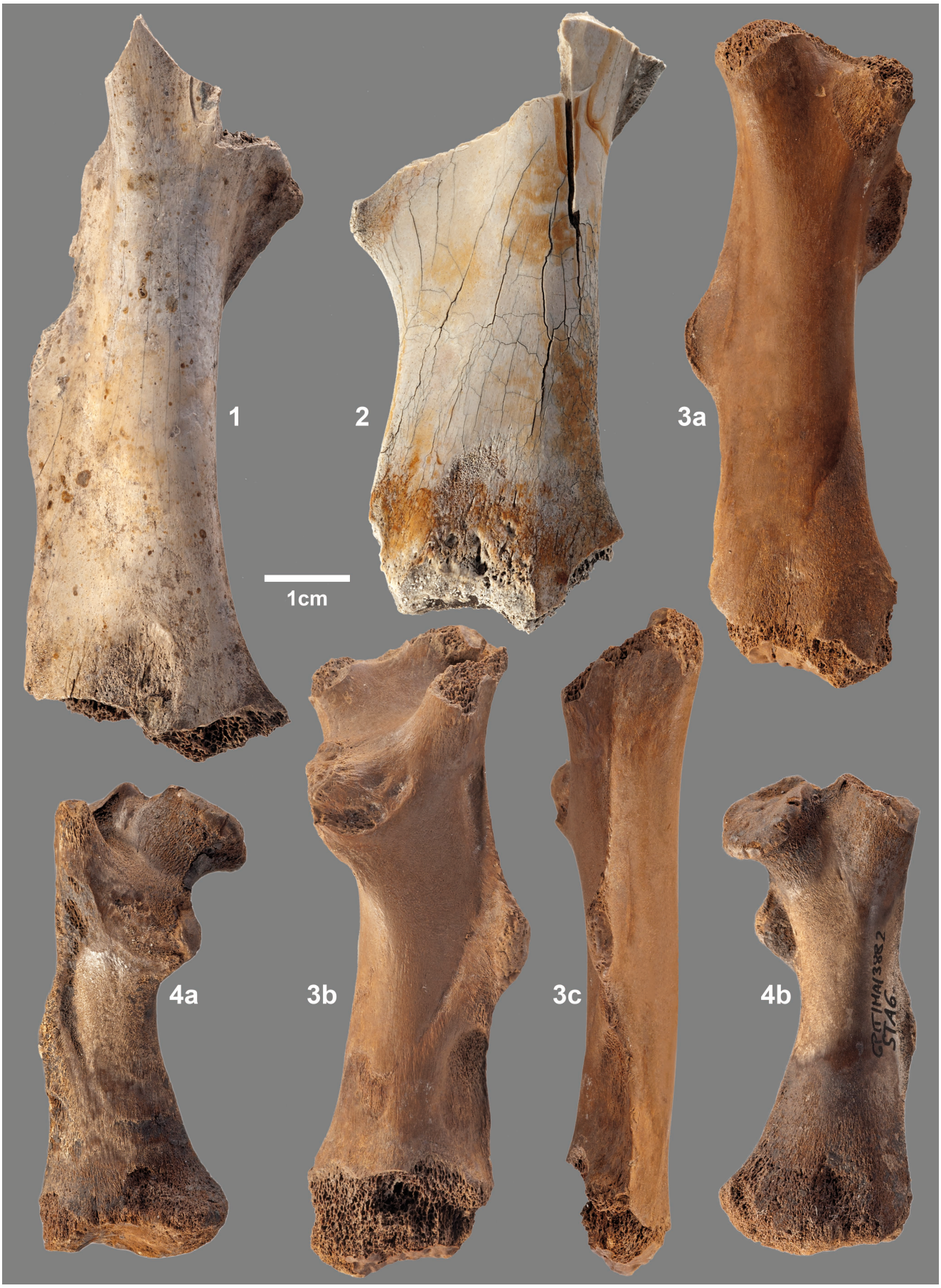
1
2
3a
1cm
4a
3b
3c
4b

PLATE 8


1a
1b
1c
GPIT/MA/09861
Sta 6-4
1cm
2a
2b
1cm
2c
2d
2e
2f
3e
3f
3a
3b
1cm
3c
3d

PLATE 10

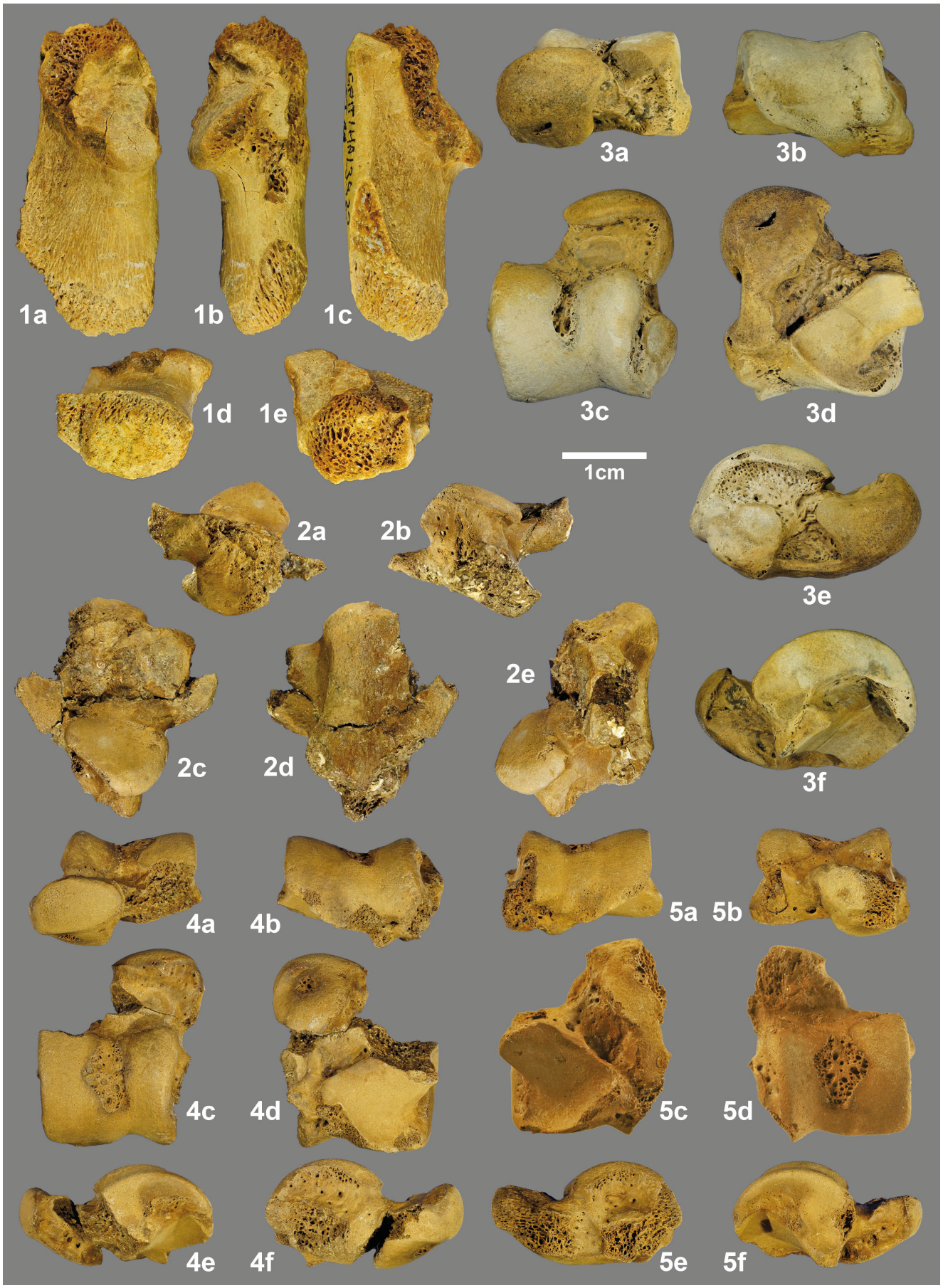
1a
1b
1c
3a
3b
3c
3d
1d
1e
1cm
2a
2b
3e
2c
2d
2e
3f
4a
4b
5a
5b
4c
4d
5c
5d
4e
4f
5e
5f

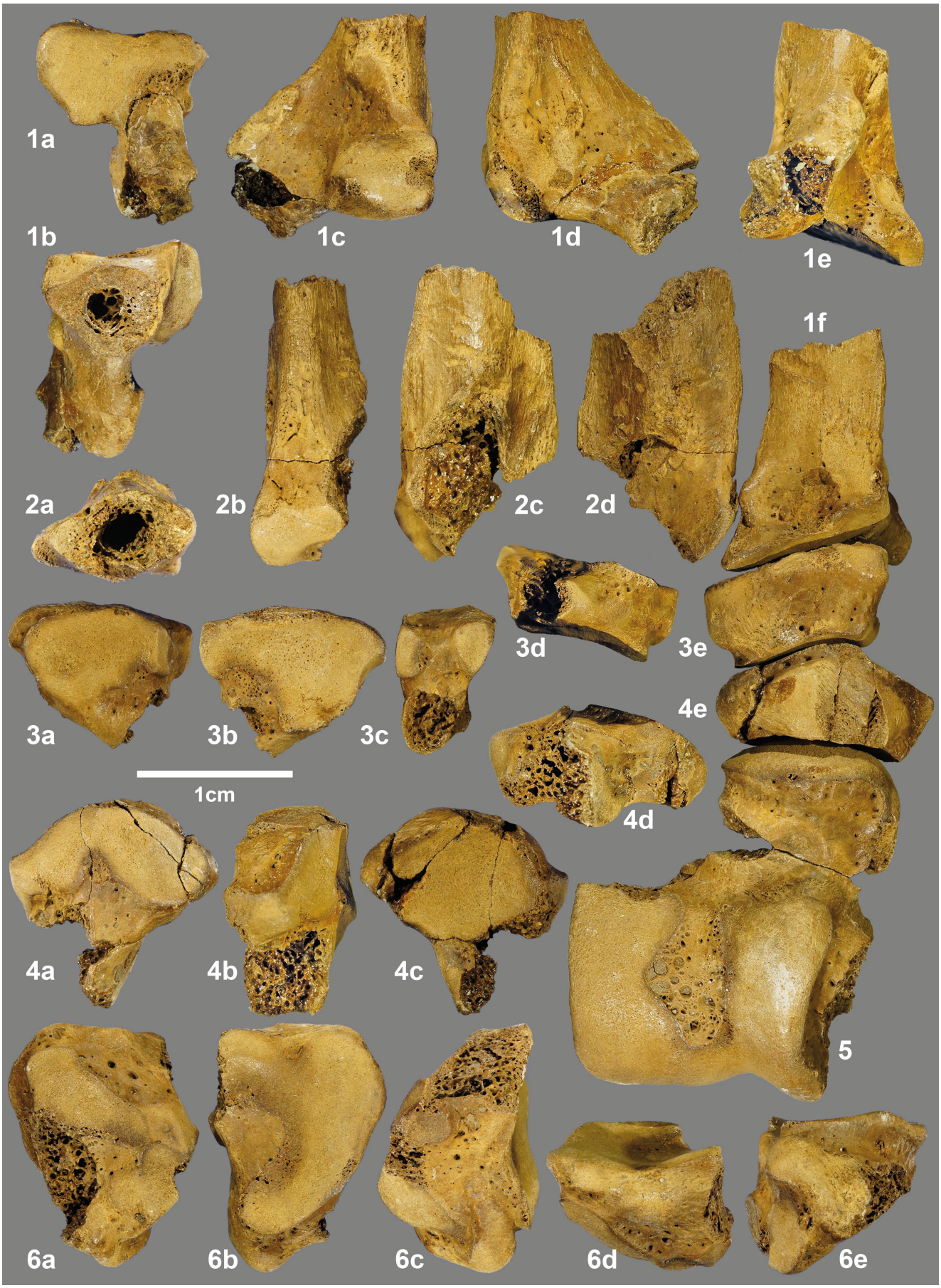
1a
1b
1c
1d
1e
1f
2a
2b
2c
2d
3a
3b
3c
3d
3e
4e
4d
1cm
4a
4b
4c
5
6a
6b
6c
6d
6e

PLATE 12

Appendix

List of all herein described postcranial bones and bone fragments representing the large Staniantsi-beaver. All specimens were found in the Staniantsi open pit coal mine and are listed with their complete informational content, including detailed stratigraphic data. “STA” is an acronym for Staniantsi and specifies the layer of sampling. (dex. = right bones; sin. = left bones).

GPIT / inventory number	Description of the specimen	Count	Stratum	Field-campaign (leg.)
GPIT/MA/03758	Ulna, sin., lacking distal end	1	STA 2	Böhme et al. 09.2012
GPIT/MA/03819	Scapula, sin., only cavitas glenoidales, proximal fragment	1	STA 6	Böhme et al. 09.2011
GPIT/MA/03822-1	Humerus, dex., shaft fragment	1	STA 6	Böhme et al. 09.2012
GPIT/MA/03822-2	Tibia, dex., distal end	1	STA 6	Böhme et al. 09.2012
GPIT/MA/03822-3	Radius, dex., lacking distal end	1	STA 6	Böhme et al. 09.2012
GPIT/MA/03822-4	Fibula, dex., lacking distal epiphysis	1	STA 6	Böhme et al. 09.2012
GPIT/MA/03822-5	Os metatarsale II, dex., lacking distal end	1	STA 6	Böhme et al. 09.2012
GPIT/MA/03822-6	Femur, caput femoris, sin., only epiphysis	1	STA 6	Böhme et al. 09.2012
GPIT/MA/03822-7	Vertebra caudalis, proximal position	1	STA 6	Böhme et al. 09.2012
GPIT/MA/03841	Phalanx distalis	1	STA 6	Böhme et al. 09.2011
GPIT/MA/03851	Vertebra caudalis, distal position	1	STA 6	Böhme et al. 09.2011
GPIT/MA/03881	Ulna, dex., proximal end	1	STA 6	Böhme et al. 09.2011
GPIT/MA/03882	Femur, sin., juvenile individual	1	STA 6, top	Böhme et al. 09.2012
GPIT/MA/03889	Phalanx distalis, digit position III or IV	1	STA 1	Böhme et al. 09.2010
GPIT/MA/03893	Vertebra caudalis, distal position	1	STA 1	Böhme et al. 09.2010
GPIT/MA/03913	Humerus, dex., shaft fragment	1	STA 1	Böhme et al. 09.2010
GPIT/MA/03922	Calcaneus, dex., fragment	1	STA 1	Böhme et al. 09.2010
GPIT/MA/09393	Pelvis, innominate bone, dex., fragment with acetabulum	1	STA 2-7	Böhme et al. 09.2014
GPIT/MA/09394	Femur, sin., only shaft	1	STA 2-8	Böhme et al. 09.2014
GPIT/MA/09409	Vertebra caudalis, proximal position	1	STA 2-7	Böhme et al. 09.2014
GPIT/MA/09468	Ulna, sin., proximal end	1	STA 2-2/3/5	Böhme et al. 06.2014
GPIT/MA/09743	Ulna, dex., proximal end	1	STA 2, centre	Böhme et al. 09.2015
GPIT/MA/09755	Femur, dex., only shaft	1	STA 2-1	Böhme et al. 09.2015
GPIT/MA/09765	Tibia, dex., distal fragment with epiphysis and fragment of the diaphysis	1	STA 1	Böhme et al. 09.2015
GPIT/MA/09767	Tibia, dex., proximal end, fragment	1	STA 2-1	Böhme et al. 09.2015
GPIT/MA/09789	Ulna, dex., proximal end	1	STA 2, top	Böhme et al. 09.2015
GPIT/MA/09793	Humerus, dex., lacking the proximal end	1	STA 1	Böhme et al. 09.2015
GPIT/MA/09794	Humerus, dex., shaft with tuberositas deltoidea, fragment	1	Stray find	Böhme et al. 09.2015
GPIT/MA/09796	Astragalus, sin., complete	1	STA 2-1	Böhme et al. 09.2015
GPIT/MA/09811	Humerus, sin., shaft, fragment	1	STA 2, top	Böhme et al. 09.2015
GPIT/MA/09823	Humerus, sin., shaft, fragment	1	STA 2-1 “Kohleblase”	Böhme et al. 09.2015
GPIT/MA/09824	Vertebra caudalis, proximal position	1	STA 2-1 “Kohleblase”	Böhme et al. 09.2015
GPIT/MA/09855	Scapula, sin., distal fragment	1	STA 6	Böhme et al. 09.2011
GPIT/MA/09856	Scapula, sin., various fragments	3	STA 2-1/9	Böhme et al. 09.2014
GPIT/MA/09858-01	Astragalus, sin., slightly damaged	1	STA 6-4	Böhme et al. 09.2012

GPIT / inventory number	Description of the specimen	Count	Stratum	Field-campaign (leg.)
GPIT/MA/09858-02	Astragalus, dex., slightly damaged	1	STA 6-4	Böhme et al. 09.2012
GPIT/MA/09858-03	Radius, dex., proximal epiphysis	1	STA 6-4	Böhme et al. 09.2012
GPIT/MA/09858-04	Humerus, distal fragment (trochlea)	1	STA 6-4	Böhme et al. 09.2012
GPIT/MA/09858-05	Calcaneus, sin., fragment	1	STA 6-4	Böhme et al. 09.2012
GPIT/MA/09858-06	Femur, dex., diaphysis, small fragment of distal epiphysis	1	STA 6-4	Böhme et al. 09.2012
GPIT/MA/09858-07	Tibia, sin., fragment	1	STA 6-4	Böhme et al. 09.2012
GPIT/MA/09858-08	Tibia, dex., fragment	1	STA 6-4	Böhme et al. 09.2012
GPIT/MA/09858-09	Scapula, dex., distal fragment	1	STA 6-4	Böhme et al. 09.2012
GPIT/MA/09858-10	Cuboideum (os tarsale IV), sin., tarsalia	1	STA 6-4	Böhme et al. 09.2012
GPIT/MA/09858-11	Naviculare, sin., tarsalia	1	STA 6-4	Böhme et al. 09.2012
GPIT/MA/09858-12	Cuneiforme 3, sin., tarsalia, ectocuneiforme, os cuneiforme laterale, third cuneiform	1	STA 6-4	Böhme et al. 09.2012
GPIT/MA/09858-13	Metatarsale IV, sin., proximal fragment, heavily damaged	1	STA 6-4	Böhme et al. 09.2012
GPIT/MA/09858-14	Metatarsale III, sin., proximal half	1	STA 6-4	Böhme et al. 09.2012
GPIT/MA/09858-15	Scapula, sin., distal fragment without joint; only spina scapulae	1	STA 6-4	Böhme et al. 09.2012
GPIT/MA/09859-1	Astragalus, dex., heavily damaged	1	STA 6-4	Böhme et al. 09.2012
GPIT/MA/09859-3	Vertebra caudalis, medial position	1	STA 6-4	Böhme et al. 09.2012
GPIT/MA/09859-4	Vertebra caudalis, proximal position	1	STA 6-4	Böhme et al. 09.2012
GPIT/MA/09859-5	Metatarsale IV, dex., proximal end	1	STA 6-4	Böhme et al. 09.2012
GPIT/MA/09861	Tibia, sin., distally slightly damaged, proximally heavily crushed	1	STA 6-4	Böhme et al. 09.2012
GPIT/MA/09931	Humerus, sin., lacking proximal end	1	STA 2, centre	Böhme et al. 09.2016
GPIT/MA/09933	Humerus, dex., distal end	1	STA 6	Böhme et al. 09.2016
GPIT/MA/09934	Femur, dex., complete	1	STA 6	Böhme et al. 09.2016
GPIT/MA/09935	Humerus, dex., complete, divided in two halfs	2	STA 2, centre	Böhme et al. 09.2016
GPIT/MA/09941	Humerus, sin., distal end	1	STA 2, stray find	Böhme et al. 09.2016
GPIT/MA/09951-3	Phalanx distalis, claw	1	STA 2, centre	Böhme et al. 09.2016
GPIT/MA/09963	Femur, dex., only shaft	1	STA 2	Böhme et al. 09.2016
GPIT/MA/09964	Ulna, sin., shaft fragment	1	STA 2, centre	Böhme et al. 09.2016
GPIT/MA/09968	Ulna, sin., distal shaft without epiphysis	1	STA 2, stray find	Böhme et al. 09.2016
GPIT/MA/10657	Tibia, dex., complete, only proximal epiphysis unfused and missing	1	STA 2, top	Böhme et al. 05.2017
GPIT/MA/10658	Calcaneus, sin.	1	STA 2, top	Böhme et al. 05.2017
GPIT/MA/10659	Metatarsale V, dex., lacking distal epiphysis	1	STA 2, centre	Böhme et al. 05.2017
GPIT/MA/10660	Humerus, dex., prox. proximal epiphysis loose, complete	2	STA 2, centre	Böhme et al. 05.2017
GPIT/MA/10663	Femur, dex., only epiphysis of the trochanter major	1	STA 2, centre	Böhme et al. 05.2017
GPIT/MA/10668	Humerus, dex., diaphysis without ends	1	STA 2-1/9	Böhme et al. 09.2014